1-2011

Recruitment of the Oncoprotein v-ErbA to Aggresomes

Cornelius Bondzi

Abigail M. Brunner

Michelle R. Munyikwa

Crystal D. Conner

et al.

See next page for additional authors

Recommended Citation

Bondzi, Cornelius; Brunner, Abigail M.; Munyikwa, Michelle R.; Conner, Crystal D.; al., et; Roggero, Vincent R.; and Allison, Lizabeth A., Recruitment of the Oncoprotein v-ErbA to Aggresomes (2011). *Molecular and Cellular Endocrinology*, 332(1-2), 196-212.
https://doi.org/10.1016/j.mce.2010.10.012

HHS Public Access

Author manuscript

Mol Cell Endocrinol. Author manuscript; available in PMC 2015 November 05.

Published in final edited form as:

Mol Cell Endocrinol. 2011 January 30; 332(0): 196–212. doi:10.1016/j.mce.2010.10.012.

Recruitment of the Oncoprotein v-ErbA to Aggresomes

Cornelius Bondzi[a], **Abigail M. Brunner**[b], **Michelle R. Munyikwa**[b], **Crystal D. Connor**[a], **Alicia N. Simmons**[a], **Stephanie L. Stephens**[b], **Patricia A. Belt**[a], **Vincent R. Roggero**[b], **Manohara S. Mavinakere**[b], **Shantá D. Hinton**[b], and **Lizabeth A. Allison**[b,*]

[a]Department of Biological Sciences, Hampton University, Hampton, VA 23668

[b]Department of Biology, College of William and Mary, Williamsburg, VA 23187

Abstract

Aggresome formation, a cellular response to misfolded protein aggregates, is linked to cancer and neurodegenerative disorders. Previously we showed that Gag-v-ErbA (v-ErbA), a retroviral variant of the thyroid hormone receptor (TRα1), accumulates in and sequesters TRα1 into cytoplasmic foci. Here, we show that foci represent v-ErbA targeting to aggresomes. v-ErbA colocalizes with aggresomal markers, proteasomes, hsp70, HDAC6, and mitochondria. Foci have hallmark characteristics of aggresomes: formation is microtubule-dependent, accelerated by proteasome inhibitors, and they disrupt intermediate filaments. Proteasome-mediated degradation is critical for clearance of v-ErbA and T_3-dependent TRα1 clearance. Our studies highlight v-ErbA's complex mode of action: the oncoprotein is highly mobile and trafficks between the nucleus, cytoplasm, and aggresome, carrying out distinct activities within each compartment. Dynamic trafficking to aggresomes contributes to the dominant negative activity of v-ErbA and may be enhanced by the viral Gag sequence. These studies provide insight into novel modes of oncogenesis across multiple cellular compartments.

Keywords

aggresome; v-ErbA; thyroid hormone receptor; cancer; misfolded protein; nucleocytoplasmic transport

1. Introduction

The retroviral Gag-v-ErbA oncoprotein ($p75^{gag\text{-}v\text{-}erb\text{-}A}$) is a highly mutated variant of the thyroid hormone receptor α1 (c-ErbA or TRα1), which is unable to bind thyroid hormone (T_3) and interferes with the action of TRα1 and the retinoic acid receptor in avian and mammalian cancer cells. Since the discovery of *v-erbA* as one of the oncogenes carried by the avian erythroblastosis virus (AEV), researchers have focused on the oncoprotein's complex mode of action in cells, with an emphasis on relating changes in amino acid sequence to its nuclear function (Beug et al., 1996; Thormeyer and Baniahmad, 1999). Theamino acid sequence changes which contribute to its oncogenic properties include fusion

*Corresponding author: Lizabeth A. Allison, Department of Biology, College of William and Mary, Integrated Science Center Room 3035B, 540 Landrum Drive, Williamsburg, VA 23187, Tele: 757-221-2232, Fax: 757-221-6483, laalli@wm.edu.

of a portion of AEV Gag to its N-terminus, N- and C-terminal deletions, and 13 amino acid substitutions. The avian *c-erbA* gene was likely fused to *gag* either by homologous recombination within the host cell genome or during retrotranscription of *c-erbA* mRNA packaged into retrovirus particles (Sap et al., 1986). For simplicity, we refer to the Gag-v-ErbA oncoprotein as v-ErbA hereinafter.

Early on, v-ErbA dominant-negative activity was attributed to competition with TRα1 for T_3-responsive DNA elements and/or auxiliary factors involved in the transcriptional regulation of T_3-responsive genes. It is now known that oncogenic conversion of v-ErbA from its cellular homolog not only involves changes in DNA binding specificity and ligand binding properties, but also the acquisition of altered nuclear export capabilities and changes in subcellular localization (Bonamy and Allison, 2006). As part of our studies, we noted that v-ErbA and other dominant negative variants of TR have a greater cytoplasmic localization compared with the wild-type receptor and often show a punctate distribution in cytoplasmic or nuclear foci (Bonamy et al., 2005; Bunn et al., 2001; DeLong et al., 2004). Even single amino acid substitutions in TR are sufficient to shift its balance to a more cytoplasmic distribution. Previously, we showed that dominant negative variants of another TR isoform, TRβ, which carry single amino acid substitutions in the DNA-binding domain (Gly121Ala and Cys122Ala), form perinuclear cytoplasmic foci (Bunn et al., 2001). Interestingly, this distribution pattern is very similar to the pattern described for a TRα dominant negative mutant in which the entire hinge, or D, domain was deleted (Lee and Mahdavi, 1993).

Upon further analysis of v-ErbA trafficking, we made a surprising discovery. Wild-type TRα1 is primarily nuclear at steady-state (Bunn et al., 2001); however, when co-expressed with v-ErbA there is a striking and dramatic shift in the distribution pattern of TRα1 (Bonamy et al., 2005). v-ErbA dimerizes with TRα1 and the retinoid X receptor, and sequesters a significant fraction of the two nuclear receptors in the cytoplasm (Bonamy et al., 2005). These results defined a new mode of action of v-ErbA, and illustrated the importance of cellular compartmentalization in transcriptional regulation (Bonamy and Allison, 2006). Our findings were closely followed by a report defining a cytoplasmic function for v-ErbA, whereby the oncoprotein sequesters Smad4 into the cytoplasm and disrupts the transforming growth factor-β (TGF-β) pathway (Erickson and Liu, 2009). To further explore the cytoplasmic activities of v-ErbA, we sought to ascertain the nature of the cytoplasmic foci formed by a subpopulation of v-ErbA.

Newly synthesized proteins must fold correctly to become functional. When the protein is misfolded, hydrophobic residues that are normally buried in the protein's interior are exposed leading to protein aggregation. Cells have evolved quality control systems that are conserved from yeast to mammalian cells to minimize protein misfolding and prevent protein aggregation (Bagola and Sommer, 2008). Molecular chaperones such as the heat shock proteins assist in refolding misfolded proteins, and bind to and stabilize exposed hydrophobic residues thereby reducing the likelihood of protein aggregation (Bercovich et al., 1997; Dul et al., 2001; Morimoto, 2008; Schroder and Kaufman, 2005). Alternatively, misfolded and aggregated proteins are destroyed by the ubiquitin-mediated proteasome degradation pathway (Pankiv et al., 2007; Ross and Poirier, 2004; Rubinsztein, 2006) or through the autophagy-lysosome system (Iwata et al., 2005; Levine and Kroemer, 2008;

Mizushima et al., 2008; Mortimore et al., 1996). Recent evidence suggests that cells have another important quality control pathway in which aggregated proteins are specifically delivered to inclusion bodies by dynein-dependent retrograde transport on microtubules. This microtubule-dependent inclusion body is called an aggresome (Garcia-Mata et al., 2002; Johnston et al., 1998; Kawaguchi et al., 2003; Kopito, 2000; Zhou et al., 2009). To promote disposal of the aggregated material, cytoplasmic aggresomes recruit chaperones and proteasomes, or trigger autophagy. In addition to waste disposal systems for the accumulation of aggregated proteins, aggresomes can also function as sites for viral replication and assembly (Wileman, 2006, 2007). Dysregulation of these mechanisms for degradation of misfolded or mutant proteins has been implicated in numerous clinical diseases, including cystic fibrosis, neurodegenerative disorders, and cancer (Heir et al., 2006; Iwata et al., 2005; Kitami et al., 2006; Ma and Lindquist, 2001; Olzmann and Chin, 2008; Riley et al., 2002; Ross and Poirier, 2004; Sha et al., 2009; Shimohata et al., 2002; Simms-Waldrip et al., 2008).

Here, we provide evidence for targeting of the oncoprotein v-ErbA to aggresomes. We have shown that v-ErbA foci display aggresomal characteristics by documenting the colocalization of v-ErbA inclusions with aggresome, proteasome, and mitochondrial markers as well as the dependence of the trafficking of these inclusions upon the dynein/dynactin motor and microtubules. Our studies offer insight into how cytoplasmic mislocalization of TRα1 by v-ErbA into aggresomes may contribute to oncogenesis. Association of a viral oncoprotein with these specialized quality control compartments provides further insight into the generality of this mechanism of aggresome trafficking for dealing with mutant proteins.

2. RESULTS

2.1 A subpopulation of the oncoprotein v-ErbA localizes to punctate foci in erythroblasts transformed with AEV

Prior studies had shown that v-ErbA expressed in transfected mammalian cell lines has a range of distributions from whole cell (with a nuclear subpopulation) to a mainly cytoplasmic distribution, localized in punctate, perinuclear foci suggestive of aggresome-like inclusions (Bonamy et al., 2005; Bunn et al., 2001). These observations raised the question of whether this localization in transfected cells adequately recapitulates the distribution of the native, virally-expressed v-ErbA. Since v-ErbA was originally isolated from chicken erythroblast cells, we used HD3 cells to investigate the distribution of native v-ErbA. HD3 cells are chicken erythroblasts transformed by AEV that express both native v-ErbA and v-ErbB (Erickson and Liu, 2009). After immunostaining with anti-v-ErbA/c-ErbA antibodies, HD3 cells were visualized by fluorescence microscopy. HD3 cells are semi-adherent cells with a rounded-up morphology and less visible cytoplasm compared with fully-adherent HeLa cells (Fig. 1). Despite these differences in morphology, cytoplasmic foci of virally-expressed v-ErbA were still readily apparent in these AEV-transformed cells (Fig. 1B). As in HeLa cells (Fig. 1A), v-ErbA was present throughout the cell, with both nuclear and cytoplasmic subpopulations. These findings thus suggest that aggresome-like inclusions are not an artefact of v-ErbA expression in transfected

mammalian cells. Similar cytoplasmic inclusions are present in AEV-infected erythroblasts, where v-ErbA acts as a potent enhancer of cellular transformation (Beug et al., 1996).

2.2 The oncoprotein v-ErbA colocalizes with aggresomal markers

Previously we showed that v-ErbA cytoplasmic foci do not represent localization of variants to membrane-bound cellular organelles and are not an artefact of the GFP tag or overexpression (Bonamy et al., 2005). To further confirm that overexpression of fluorescent protein-tagged fusion proteins does not lead to aggresome formation by a non-specific mechanism, we tested a panel of fluorescent proteins for their localization after transfection into HeLa cells (Fig. 2A). No cytoplasmic foci were observed for any of the fluorescent proteins or tagged fusion proteins analyzed. GFP, DsRed2, and Dendra were distributed diffusely throughout the whole cell; the fusion protein GFP-GST-GFP was diffusely distributed throughout the cytoplasm; and, in the absence of ligand, GFP-tagged glucocorticoid receptor was localized primarily to the cytoplasm in a diffuse distribution pattern.

These findings point to the possibility that cytoplasmic foci could represent specific targeting of v-ErbA to aggresomes. Besides aggresome formation, other protein aggregation pathways also appear to exist in mammalian cells (Zaarur et al., 2008). Thus, to confirm that v-ErbA aggregates are bona fide aggresomes, we conducted definitive cotransfection assays with fluorescently-tagged fusion proteins. Cytoplasmic foci were observed for DsRed2-tagged v-ErbA, as well as for v-ErbA tagged with Dendra2, a monomeric fluorescent protein (Fig. 2B).

Characteristics of aggresomes are portrayed by the protein chimeras GFP-250 and GFP170*. GFP-250 is composed of GFP fused at its C-terminus to the first 250 amino acids of p115, a protein involved in the transport of cargo from the endoplasmic reticulum to the Golgi (Nelson et al., 1998). GFP170* is composed of GFP fused to amino acids 566–1375 of the Golgi Complex Protein (GCP)-170 (Fu et al., 2005; Hicks and Machamer, 2002). In previous studies, overexpression of GFP-250 was shown to result in a spherical aggregate at the MTOC, similar to those formed by other cellular proteins (Garcia-Mata et al., 1999). We observed comparable aggregates in HeLa cells transfected with GFP-250 expression plasmid (Fig. 2C). To investigate whether or not the foci formed by v-ErbA colocalized with aggresomal markers, HeLa cells were cotransfected with GFP-250 and DsRed2-tagged v-ErbA expression plasmids and their subcellular localizations were observed (Fig. 2D). Cells were fixed both 24 h and 48 h post-transfection to observe the dynamics of aggresome formation. After 24 h, cells cotransfected with DsRed2-v-ErbA and GFP-250 contained smaller more dispersed aggregates of both proteins throughout the cytoplasm. There was a high degree of colocalization between these small aggregates, suggesting that both of these proteins follow the same dynamic pathway. After 48 h, the cells contained larger coalesced aggregates of both GFP-250 and DsRed2-v-ErbA. DsRed2-v-ErbA and GFP-250 completely colocalized in 59 ± 4% of cells and partially colocalized in 38 ± 4% of cells (Fig. 2D and 2E). These results strongly suggest that DsRed2-v-ErbA and GFP-250 are targeted to the same subcellular compartment, despite their slight differences in morphology. In contrast to GFP 250, GFP170* forms large “ribbon-like” aggregates at the MTOC and punctate foci in

the nucleus (Fu et al., 2005). These nuclear inclusions codistribute with promyelocytic leukemia (PML) bodies and have been referred to as nuclear aggresomes (Fu et al., 2005). DsRed2-v-ErbA also colocalized with the cytoplasmic aggregates formed by GFP170* (Fig. 2D). Taken together, these data provide strong evidence for association of v-ErbA with aggresomes.

2.3 Formation and movement of v-ErbA inclusions is microtubule- and dynein-dependent

After demonstrating that v-ErbA colocalized with the aggresomal markers GFP-250 and GFP170*, we next sought to ascertain whether v-ErbA foci possess other hallmark characteristics of aggresomes. Aggresome formation occurs when small aggregates of misfolded and defective proteins travel in a minus-end direction along the microtubule tracks towards the MTOC. Thus, microtubule disruption by the drug nocodazole prevents bona fide aggresome formation (Fu et al., 2005; Garcia-Mata et al., 1999; Garcia-Mata et al., 2002).

Nocodazole disrupts microtubules by preventing their polymerization. The drug binds to a sulfhydryl group on β-tubulin, prevents disulfide linkages with additional tubulin heterodimers and inhibits transport of cargo and cell division (Luduena and Roach, 1991; Vasquez et al., 1997). First, to confirm that nocodazole had an inhibitory effect upon the microtubule network in our system, untransfected cells were either treated with nocodazole or DMSO (vehicle control), or left untreated. The cells were then stained with anti-β-tubulin to visualize the microtubules. Cells that were untreated or treated with DMSO displayed a fibrous, wispy network of microtubules that spanned the whole cell (Fig. 3A). However, those cells that had been treated with nocodazole lacked the fibrous network that existed in untreated cells, indicating that the microtubule network was disrupted.

Next, to determine whether the disruption of microtubules would prevent the formation of the coalesced foci, 16 h post-transfection HeLa cells expressing GFP-v-ErbA were treated with nocodazole for 20 h. If aggresome formation was inhibited, one would expect to see a diffuse expression pattern or a dispersal of small aggregates throughout the cytoplasm. As predicted, treatment of GFP-v-ErbA-expressing cells with nocodazole resulted in a majority of cells with a diffuse pattern of v-ErbA expression (Fig. 3B). Only 13 ± 3% of untreated cells contained diffuse aggregates (Fig. 3C). Upon nocodazole treatment, there was a significant shift ($p<0.001$) to 55 ± 3% of cells containing diffuse aggregates. While 46 ± 5% of untreated v-ErbA-expressing cells contained large aggregates, only 7 ± 3% of nocodazole-treated cells had large aggregates. Because nocodazole cannot disrupt aggregates that are already intact prior to treatment, many of the aggregates observed in treated cells could have been preexisting. Movement of v-ErbA pre-aggresomal structures to the nuclear periphery was also demonstrated by live cell imaging (see Video S2 in the supplemental material). Taken together, data thus suggest that over time, v-ErbA aggregates are transported via microtubule motors and coalesce in a perinuclear structure.

The dynein/dynactin complex serves as a minus-end (retrograde) directed motor that transports cargo, including aggregates of misfolded proteins, along the microtubule tracks from the cell periphery to the MTOC. Aggresomes form when these smaller aggregates reach the MTOC (Melkonian et al., 2007). Dynactin is a multiprotein complex that is

required for the majority of dynein-based movement *in vivo*. One subunit of dynactin, p50/dynamitin, is directly involved in the attachment of cargo to dynein. Overexpression of p50/dynamitin is known to dissociate the dynein/dynactin complex and, thereby, reduces the extent of aggresome formation and sequesters proteins into pre-aggresomal structures (Garcia-Mata et al., 2002; Johnston et al., 2002; Melkonian et al., 2007; Sha et al., 2009). Thus, disruption of the formation of v-ErbA foci by overexpression of p50/dynamitin would provide further evidence of the aggresomal nature of these aggregates.

Cells were transfected with GFP-250 as a control or GFP-v-ErbA expression plasmid, either alone or together with p50/dynamitin expression plasmid. Consistent with published reports (Garcia-Mata et al., 2002), 27% of cells expressing GFP-250 alone contained fully formed aggresomes, while 73% contained small aggregates (Fig. 3D and 3E). In contrast, 13% of cells cotransfected with GFP-250 and p50/dynamitin expression plasmids contained fully-formed aggresomes and 87% contained small aggregates.

Similar to the pattern observed for GFP-250, 49% of cells expressing v-ErbA alone contained aggresomes, while 51% contained small aggregates (Fig. 3F and 3G). In contrast, approximately 26% of cells cotransfected with GFP-v-ErbA and p50/dynamitin expression plasmids contained aggresomes and 74% contained small aggregates. Taken together, these findings provide evidence that formation of v-ErbA-containing aggresomes is mediated by the dynein/dynactin motor protein complex.

2.4 v-ErbA inclusions cause a disruption of vimentin intermediate filaments and recruit histone deacetylase 6 (HDAC6)

A number of aggresome-forming misfolded proteins and viral particles have been shown to cause a collapse of the intermediate filament meshwork composed of vimentin into a circular vimentin “cage” around the area of aggregated protein for immobilization and containment (Fu et al., 2005; Garcia-Mata et al., 1999; Heath et al., 2001; Johnston et al., 1998). Since v-ErbA has a more “ribbon-like” (as defined by Fu *et al.*, 2005) morphology in the absence of proteasome inhibition, the formation of a circular “cage” around the area of aggregated protein was not predicted. To determine whether v-ErbA foci caused some type of disruption of vimentin, cells transfected with GFP-v-ErbA were stained with a Cy3-conjugated antibody against vimentin 48 h post-transfection. In untransfected cells, the vimentin distribution pattern was filamentous and dispersed throughout the cell (Fig. 4A). However, cells transfected with GFP-v-ErbA showed a reorganization and collapse of vimentin filaments around the area of aggregated protein (Fig. 4B). These results provide additional evidence that v-ErbA foci exhibit aggresomal characteristics.

Dynein-mediated transport of cargo to aggresomes is necessary for their formation. In some cases aggresomes also appear to become enriched in dynein (Diaz-Griffero et al., 2006; Johnston et al., 2002; Szebenyi et al., 2007). Thus, we tested for colocalization of the aggresomal marker GFP-250 (Fig. 4C) and GFP-v-ErbA (Fig. 4D) with dynein, by immunostaining of transfected cells with anti-dynein antibodies. Some cells were treated with the proteasome inhibitor MG132 for 20 h prior to fixation, in order to increase the amount of mature aggresome formation compared to pre-aggresomal structures in untreated cells (Fig. 4C and 4D, lower panels). No distinct colocalization was observed between

GFP-250 or GFP-v-ErbA and dynein in either untreated or MG132-treated cells. Data thus suggest that for these particular cargo types, the dynein/dynactin motor complex does not accumulate in aggresomes to any significant degree.

We next sought to ascertain whether v-ErbA inclusions colocalize with the tubulin deacetylase, histone deacetylase 6 (HDAC6), another key marker characteristic of aggresomes (Boyault et al., 2007; Iwata et al., 2005; Rodriguez-Gonzalez et al., 2008). Most HDACs are localized to the nucleus and play a role in transcriptional repression (Suzuki, 2009). HDAC6 is unusual in that it is localized to the cytoplasm and mediates deacetylation of non-histone proteins, including α-tubulin (Olzmann and Chin, 2008; Sha et al., 2009). Of the eighteen HDACs identified so far, only HDAC6 has been shown to be involved in regulation of aggresome function (Suzuki, 2009).

To investigate whether or not GFP-250 and GFP-v-ErbA-containing aggresomes colocalized with HDAC6, HeLa cells were transfected with either GFP-250 or GFP-v-ErbA expression vectors. Twenty four hours post transfection, cells were fixed and stained with anti-HDAC6 antibodies and the subcellular localizations of proteins were observed. Colocalization with a subpopulation of HDAC6 was evident in GFP-250-expressing cells that contained fully-formed aggresomes (Fig. 4E). Colocalization with a subpopulation of HDAC6 was also observed in cells expressing GFP-v-ErbA (Fig. 4F); correlating with the formation of large, perinuclear aggresomes.

2.5 Proteasome inhibition enhances the size of v-ErbA aggresomes but does not induce cytoplasmic aggregates of TRα1

The inhibition of proteasome activity typically leads to an increase in aggresome size (Fu et al., 2005; Garcia-Mata et al., 1999; Johnston et al., 1998). To determine whether the size of v-ErbA foci would increase in response to proteasome inhibition, cells expressing GFP-v-ErbA were treated 16 h post-transfection with the proteasome inhibitor MG132 for 20 h. MG132 blocks proteasome degradation by inhibiting the chymotrypsin-like activity of the proteasome, preventing the cleavage of peptide bonds within the target protein (Lee and Goldberg, 1998).

As predicted, MG132 treatment dramatically increased the size of v-ErbA foci. Interestingly, most of the large aggregates were spherical in morphology and coalesced into a single aggregate (Fig. 5A, right panel), similar to the spherical aggresomes formed by GFP-250, mutant huntingtin protein (Kuemmerle et al., 1999) and mutant cystic fibrosis transmembrane conductance regulator (CFTR) (Johnston et al., 1998) after proteasome inhibition. In contrast, in the absence of MG132, v-ErbA inclusions were “ribbon-like” (as defined by Fu *et al.*, 2005) in morphology or consisted of multiple, smaller aggregates (Fig. 5A, left panel). Since improper folding of proteins can occur as a result of high levels of protein expression (Olzmann and Chin, 2008), we also analyzed the localization of GFP. No foci or aggregates were seen in cells expressing GFP alone, although there was a slight increase in the intensity of GFP fluorescence in cells treated with MG132 (data not shown).

In addition to an increase in the size of aggregates, v-ErbA-expressing cells treated with MG132 showed more intense fluorescence when compared with untreated cells, suggesting

that there was an increase in cellular levels of v-ErbA as a result of inhibition of proteasome activity. Quantification of replicate experiments showed that only 41 ± 2% of untreated cells contained large aggregates of GFP-v-ErbA, but upon MG132 treatment, there was a significant shift ($p<0.001$) to 78 ± 7% of v-ErbA-expressing cells containing large aggregates (Fig. 5B).

To confirm that the increase in v-ErbA aggregate size was due to an increase in total protein and not just the coalescence of pre-existing smaller aggregates, we carried out immunoblot analysis of v-ErbA expression levels in HeLa cells. Immunoblot analysis showed a greater accumulation of GFP-v-ErbA in MG132-treated transfected cells compared with untreated (Fig. 5C). Taken together, these results suggest that the proteasome machinery normally degrades some of the aggregated v-ErbA, thus preventing formation of mature aggresomes in all cells.

In contrast to the oncoprotein v-ErbA, cytoplasmic foci are not observed when the cellular homolog TRα1 is over-expressed in mammalian cells (Bonamy et al., 2005). For some other proteins, such as malin and laforin, where <8% of transfected cells show aggregates, proteasome inhibition is required to induce formation of aggregates (Mittal et al., 2007). Thus, we sought to ascertain whether treatment with MG132 would induce cytoplasmic inclusions of TRα1. Prior studies have shown that T_3-binding induces rapid proteasome-mediated degradation of endogenous or untagged, exogenous TRα1 in GC cells (growth hormone-producing rat pituitary tumor cell line) (Dace et al., 2000) and in cardiomyocytes (Kenessey and Ojamaa, 2005). This mechanism of receptor downregulation appears to be conserved among the nuclear receptor superfamily and has been proposed to be an important mechanism by which receptor signaling can be regulated (Kenessey and Ojamaa, 2005). To determine whether GFP-tagged TRα1 is also subject to proteasome-mediated degradation, we carried out both *in situ* and immunoblot analysis in HeLa cells.

Immunoblot analysis showed a greater accumulation of GFP-TRα1 in MG132-treated transfected cells compared with untreated (Fig. 5D). Strikingly, proteasome-mediated degradation of GFP-tagged TRα1 was much more rapid in cells treated with T_3 than in the absence of hormone. Thyroid hormone had no effect on GFP-v-ErbA and EGFP turnover rates (data not shown). For analysis of proteasome-mediated degradation of TRα1 *in situ*, cells were transfected with expression vectors for GFP-TRα1. Cells treated with T_3 showed much fainter nuclear fluorescence of GFP-TRα1 compared with untreated cells (Fig. 5E). In contrast, cells treated with proteasome inhibitor had a greater level of protein expression and often had large foci within the nucleus (Fig. 5F). Taken together, these findings indicate that like the oncoprotein v-ErbA, TRα1 undergoes proteasome-mediated degradation, and that degradation of TRα1 is much more rapid in the presence of ligand. However, treatment with MG132 does not induce cytoplasmic inclusions of TRα1.

2.6 v-ErbA aggresomes recruit proteasomes and cellular chaperones

Formation of aggresomes has been reported to involve the recruitment of cytosolic components, including chaperones, ubiquitination enzymes, and proteasome subunits, to facilitate clearance of aggregated proteins (Fu et al., 2005; Garcia-Mata et al., 2002; Mittal et al., 2007; Waelter et al., 2001); however, this proteasome recruitment does not necessarily

require ubiquitination of aggresome components (Garcia-Mata et al., 2002). To further characterize foci formed by v-ErbA as aggresomes, we investigated the association of proteasomes, Hsp70 and ubiquitin with v-ErbA.

To investigate GFP-v-ErbA cytoplasmic inclusions and their potential colocalization with proteasomes, we transfected cells with expression vectors for either GFP-250 or GFP-v-ErbA (Fig. 6A). After immunostaining with anti-20S proteasome subunit antibodies (the catalytic core of the 26S proteasome), cells were observed by fluorescence microscopy. Some cells were treated with MG132 in order to increase the amount of mature aggresome formation compared to pre-aggresomal structures in untreated cells. We first investigated the colocalization of the aggresomal marker GFP-250 with proteasomes. 20S proteasome subunits showed a diffuse distribution throughout the cytoplasm; however, 59% of cells with GFP-250 aggregates displayed distinct colocalization of a subpopulation of 20S proteasome subunits with these aggregates (Fig. 6A, upper panels). Of the cells that were overexpressing GFP-v-ErbA, 68% of those that formed aggresomes showed colocalization with a subpopulation of 20S proteasome subunits (Fig. 6A, lower panels).

To investigate GFP-v-ErbA cytoplasmic inclusions and their colocalization with Hsp70 and ubiquitin, Hela cells were transiently transfected with either expression vectors for GFP-250 or GFP-v-ErbA, and immunostained with antibodies specific for hsp70 or ubiquitin (Fig. 6B and 6C). To maximize aggresome formation, a portion of the cells were also treated with the proteosome inhibitor MG132. A subpopulation of Hsp70 colocalized with GFP-250 and GFP-v-ErbA in the presence or absence of MG132 in cells with aggregated foci (Fig. 6B). Our results showing colocalization of hsp70 with GFP-250 are consistent with the previously reported observations by Garcia-Mata *et al.* (1999), and are consistent with other published data on the recruitment of hsp70 as well as other classes of molecular chaperones to aggresomes (Garcia-Mata et al., 1999; Wigley et al., 1999). Colocalization of hsp70 with GFP-v-ErbA therefore provides additional evidence that foci formed by v-ErbA are aggresomes.

Ubiquitin was not observed to colocalize with either GFP-250 or GFP-v-ErbA (Fig. 6C). There are inconsistent reports of ubiquitin localization to aggresomes. GFP-250 forms aggresomes without being ubiquitinated (Garcia-Mata et al., 1999; Kawaguchi et al., 2003); likewise superoxide dismutase (SOD)-containing aggresomes do not appear to contain ubiquitinated proteins (Johnston et al., 2000). Aggresomes formed in cells expressing CFTR (Johnston et al., 1998) (Wigley et al., 1999); influenza virus nucleoprotein (Antón et al, 1999), mutant surfactant protein C (Kabore et al., 2001), malin and laforin (Mittal et al., 2007), and rhodopsin (Saliba et al., 2002) do, however, react with antibodies to polyubiquitin, suggesting that proteins within these inclusions are ubiquitinated. Our findings that neither GFP-250 nor GFP-v-ErbA colocalize with ubiquitin, further indicate that ubiquitin may not always be a requirement for aggresome formation or protein turnover by this pathway. The variability in the association of ubiqutin with aggresomes as reported may also suggest substrate-specific recruitment of components of the protein degradation and folding machinery.

2.7 Mitochondria are recruited to v-ErbA aggresomes

Microtubules provide the tracks for intracellular trafficking and regulate the distribution of cellular organelles, which are normally localized throughout the cytosol. The accumulation of aggregrated proteins causes disorganization of the microtubule network and leads to retraction of mitochondria from the cell periphery to the area of the aggresome and viral replication factories (Bauer and Richter-Landsberg, 2006; Heath et al., 2001; Mittal et al., 2007; Muqit et al., 2006; Nozawa et al., 2004; Wileman, 2007). It is hypothesized that mitochondria are recruited to aggresomes to provide energy for the processes of protein folding and/or protein degradation (Waelter et al., 2001). Both the 20S proteasome subunit and chaperones have been shown to localize to the aggresome (Garcia-Mata et al., 1999) (and this paper). These structures both require the use of ATP to function; thus, it is plausible that mitochondria are retracted towards aggresomes to provide energy.

Colocalization of mitochondria with GFP-250 and GFP-v-ErbA aggresomes and pre-aggresomal structures was assessed by staining cells with MitoTracker Red, a mitochondrion-selective dye. Mitochondria were distributed throughout the cytosol of untransfected cells (Fig. 7A), and in cells transfected with expression vectors for EGFP (Figure 7B) and GFP-TRα1 (Fig. 7C), as a control. In striking contrast, in 61% of cells that formed GFP-250 aggresomes, these foci colocalized with clusters of mitochondria that were retracted from the cell periphery (Fig. 7D).

In a prior study, when we analyzed cells where v-ErbA was present in punctate foci throughout the cytoplasm, we did not detect colocalization of these pre-aggresomal inclusions of v-ErbA with mitochondria (Bonamy *et al.*, 2005). However, since our prior analysis did not examine mature, fully-formed aggresomes, we re-visited the question of colocalization of v-ErbA-containing aggresomes with mitochondria. Here, we observed colocalization of v-ErbA with mitochondria in 83% of cells that formed mature aggresomes (Fig. 7E). These findings indicate that both GFP-250 and GFP-v-ErbA aggresomes recruit mitochondria.

2.8 Deletion of the Gag sequence leads to nuclear retention of v-ErbA and decreases the recruitment of v-ErbA to aggresomes

Many viruses replicate in intracellular compartments, which are thought to increase efficiency of replication by isolating the viral components. These compartments, known as viral factories, are similar to aggresomes in that they rearrange vimentin, travel along the microtubule tracks, converge at the MTOC, and recruit chaperones, ubiquitin, and mitochondria (Arnaud et al., 2007). Additionally, the formation of viral factories, like aggresomes, is inhibited by the overexpression of p50/dynamitin and treatment with nocodazole (Wileman, 2006). Because v-ErbA is a retroviral oncoprotein, studying its cytoplasmic inclusions offers valuable insight in the study of both aggresomes and viral factories. As noted earlier, v-ErbA is expressed by AEV as a Gag-v-ErbA fusion protein (Sap et al., 1986). The Gag sequence is required for the biological activity of the oncoprotein (Erickson and Liu, 2009), and it contains a strong nuclear export sequence (DeLong et al., 2004). In a virus, Gag is involved in forming the viral capsid. Thus, it is possible that the Gag sequence serves as an aggresome targeting sequence; like other viral

components, it may be recognized by the dynein motors, which carry the protein along the microtubule tracks towards the nucleus.

To investigate the role of the Gag sequence in the subcellular localization of v-ErbA, cells were transiently transfected with GFP-ΔGag-v-ErbA (Gag sequence deleted) and viewed by fluorescence microscopy (Fig. 8A). Greater than 50% of cells expressing GFP-v-ErbA (containing Gag sequence) contain large cytoplasmic inclusions (e.g. see Fig. 3). In contrast, ΔGag-v-ErbA showed a significant nuclear population, a much more diffuse cytoplasmic distribution (Fig. 8B), and only a small percentage of cells (~1%) showed foci within the cytoplasm (Fig. 8C, also compare Fig. 8A with Figs. 1A and 2B). However, of these cells with cytoplasmic foci, 93.5% showed colocalization of TRα1 with ΔGag-v-ErbA in cells co-expressing mCherry-tagged TRα1 and GFP-ΔGag-v-ErbA (Fig. 8C and 8D). These findings are consistent with our prior studies reporting that v-ErbA sequesters TRα1 in cytoplasmic foci by forming heterodimers (Bonamy et al., 2005).

Interestingly, YFP-tagged Gag (1–70), which localizes entirely to the cytoplasm (DeLong et al., 2004), formed multiple foci in the cytoplasm of 30% of cells. Thus, it is possible that the N-terminal 70 amino acids of AEV Gag may play a role in promoting the formation of these cytoplasmic foci also characteristic of v-ErbA. However, Gag alone is unable to sequester TRα1 in foci, presumably because Gag and TRα1 do not physically interact *in situ*. In cells co-expressing mCherry-TRα1 and YFP-Gag (1–70) there was no colocalization of the two proteins (Fig. 8C and 8E). YFP-Gag (1–70) remained localized to the cytoplasm and TRα1 remained localized to the nucleus. Although the Gag protein does appear to contribute to the cytoplasmic localization of v-ErbA and its recruitment to aggresomes, our data indicate that it is not the only contributing factor. When Gag is deleted, v-ErbA becomes more localized to the nucleus and, as a consequence, less of the oncoprotein is available for aggresome formation because of its altered distribution.

2.9 Dynamics of v-ErbA aggresome formation

Although mainly cytoplasmic at steady-state, it is well documented that v-ErbA has a nuclear function and undergoes nucleocytoplasmic shuttling (Bonamy et al., 2005; Bunn et al., 2001; DeLong et al., 2004). Leptomycin B (LMB), a specific inhibitor of the export receptor CRM1/exportin 1 (Kutay and Güttinger, 2005), blocks nuclear export of v-ErbA; LMB treatment results in complete nuclear localization of v-ErbA, indicating that v-ErbA utilizes a CRM1-dependent nuclear export pathway (Bunn et al., 2001). We were thus interested in understanding the movements of v-ErbA between cytoplasmic subcompartments and the nucleus. To determine the dynamics of aggresome formation by v-ErbA, we investigated aggresome formation reversibility (Fig. 9). After treatment with LMB for 5 h, pre-existing cytoplasmic foci disappeared and GFP-v-ErbA showed a primarily nuclear localization in 87% of cells in a time dependent manner, suggesting that aggresome formation is dynamic and reversible (compare Fig. 9A and 9C with Fig. 9B and 9D). The number of cells with aggregates remained constant over time in untreated cells; whereas, the number of cells with aggregates decreased dramatically in cells treated with LMB (Fig. 9E), correlating with nuclear accumulation of v-ErbA.

These studies were carried out on cells fixed at specific time points, thus it was not possible to track the fate of a particular cell. To further investigate the dynamics at single-cell resolution, we carried out kinetic experiments in live cells. Real time analysis in living cells confirmed that aggregates were highly mobile; there was disappearance of small aggregates and diffuse accumulation of v-ErbA in the nucleus in the presence of LMB (Fig. 9F, supplementary Video S1); however, large aggregates did not dissociate and typically during the time course for cells with large aggregates, cell death occurred (Fig. 9G, supplementary Video S2). These findings suggest that small aggregates are mobile and reversible, but formation of mature aggresomes is an end-point.

3. Discussion

Previously we showed that a subpopulation of the v-ErbA oncoprotein (Gag-v-ErbA) accumulates in cytoplasmic foci and sequesters a significant fraction of TRα1 in these foci in transfected mammalian cells, contributing to its oncogenic properties (Bonamy and Allison, 2006; Bonamy et al., 2005). Here, we show that cytoplasmic foci are also present in chicken erythroblasts that are transformed with AEV and express native v-ErbA. We show that these foci represent targeting of v-ErbA to classic aggresomes. v-ErbA foci colocalize with aggresomal markers, are dependent on microtubule transport for their formation, disrupted the intermediate filament meshwork composed of vimentin and were enhanced in size upon treatment with proteasome inhibitors. Our studies thus highlight the complexity of v-ErbA's mode of action. v-ErbA is a highly mobile protein that trafficks between multiple cellular compartments and carries out distinct activities within each compartment. The first two compartments are well-documented in the literature: a diffuse cytosolic location where v-ErbA is thought to dysregulate the mTOR (mammalian target of rapamycin) and TGF-β pathways (Erickson and Liu, 2009; Gonin-Giraud et al., 2008) and a nuclear location where it interacts with target genes (Bresson et al., 2007; Ventura-Holman et al., 2008). The third compartment, described here, is a perinuclear inclusion characterized as an aggresome. In addition to contributing to its dominant negative activity, trafficking of v-ErbA to aggresomes may play a role in turnover of the oncoprotein or, in the complete retrovirus, in viral replication and assembly.

3.1 Dynamics and morphology of v-ErbA aggresomes

A striking feature of v-ErbA foci is their highly mobile nature as they move along microtubule tracks, and the appearance and disappearance of small aggregates. Other proteins have also been shown to exchange rapidly between aggregates and a soluble pool (Fu et al., 2005; Mignot et al., 2007; Opazo et al., 2008). Importantly, we observed the disappearance of small v-ErbA aggregates in cells treated with the nuclear export inhibitor LMB, whereas cells with large perinuclear aggresomes typically underwent cell death during imaging. These observations of aggresome dynamics provide a plausible explanation for the apparent absence of fully-formed v-ErbA aggresomes in HD3 cells. It is likely that there is some mechanism in this AEV-transformed erythroblast cell line to prevent large aggregates from forming, thus allowing these cells to continue to proliferate in culture.

Aggresome formation is generally categorized into two broad categories: spherical (Garcia-Mata et al., 1999; Garcia-Mata et al., 2002; Heath et al., 2001; Johnston et al., 1998;

Kuemmerle et al., 1999), or “ribbon-like” (Ardley et al., 2004; Fu et al., 2005; Mignot et al., 2007). The criteria for formation of either of these two distinct morphologies have yet to be determined. v-ErbA inclusions typically formed a “ribbon-like” shape, but coalesce into a more spherical shape in cells treated with MG132. Spherical aggresomes formed by mutant CFTR also are only observed when induced by proteasome inhibitors (Johnston et al., 1998). These results suggest that the final aggresomal morphology for v-ErbA is not always reached after 48 h in cells with active proteasomes. Regardless of the effect on aggregate morphology, it is evident from the results presented here that protein degradation by the proteasome is critical for clearance of v-ErbA from the cell, as well as for the T_3-dependent clearance of TRα1.

Trafficking of v-ErbA aggregates occurs by microtubule-mediated transport. HDAC6 may act as an adaptor protein linking polyubiquinated proteins to the dynein motor complexes for transport (Sha et al., 2009). However, we did not detect ubiquitin or dynein in v-ErbA aggresomes. The question thus remains of why HDAC6 is present in v-ErbA aggresomes. In addition to its function as an adaptor, HDAC6 has also been shown to deacetylate hsp90 and modulate its chaperone activity (Boyault et al., 2007). Hsp90 also partially co-localizes with aggresomes (Diaz-Griffero et al., 2006), and is known to form cytoplasmic complexes with v-ErbA (Privalsky, 1991), thus colocalization of HDAC6 with v-ErbA aggresomes could be due to association with hsp90 as opposed to interaction with ubiquitinated proteins and dynein. It remains to be determined whether this is the case.

3.2 Significance of targeting of v-ErbA to aggresomes

Targeting of v-ErbA to aggresomes may be a cellular response to the accumulation of the oncoprotein in the cytoplasm, thus serving as a quality control mechanism to sequester the mutant protein for turnover and disposal by the proteasome machinery. Our data show that mitochondria are recruited to v-ErbA aggresomes, raising some intriguing questions about the functional significance of such recruitment. It is hypothesized that mitochondria are recruited to aggresomes to provide energy for the processes of protein folding and/or protein degradation (Waelter et al., 2001). Alternatively, this retraction of mitochondria from the cell periphery could be a side-effect of disorganization of the cytoskeleton, due to vimentin redistribution.

Both the 20S proteasome subunit and chaperones have been shown to localize to the aggresome (Garcia-Mata et al., 1999) (and this paper); however, proteasome-mediated degradation is not thought to be very efficient at the aggresome (Garcia-Mata et al., 2002). Autophagy has been proposed to be a more effective system for degradation; however, autophagy-mediated clearance of aggresomes is not a universal phenomenon and appears to be dependent on the nature of the cytoplasmic inclusions (Wong et al., 2008). Ultimately, cells might undergo cell death if there is too great an accumulation of aggregated protein, as reported for cells containing mutant glial fibrillary acidic protein (GFAP) aggregates (Mignot et al., 2007), and as observed in our time-lapse recordings of v-ErbA dynamics. Clustering of mitochondria around aggresome-like structures may also coincide with markers of apoptosis in the cell (Cereghetti and Scorrano, 2006; Debure et al., 2003; Soo et

al., 2009). Thus, it is possible that mitochondria, once present at the MTOC, engage in signaling pathways that promote apoptosis.

Alternatively, recruitment of v-ErbA to aggresomes could be a remnant viral behavior for assembly at a viral factory. It is possible that a cellular response originally designed to reduce the potential toxicity of misfolded proteins is exploited by viruses as a means of concentrating structural proteins at sites of virus assembly (Prichard et al., 2008; Wileman, 2006). Aggresome-forming viral factories have been shown to colocalize with the aggresomal marker GFP-250, disrupt vimentin intermediate filaments, and depend on intact microtubules for their formation, consistent with the properties of v-ErbA foci (Arnaud et al., 2007; Heath et al., 2001; Liu et al., 2005). The retroviral oncoprotein v-ErbA is a fusion protein that contains a portion of the AEV Gag sequence, which encodes structural proteins involved in the formation of the viral capsid. Prior studies in our lab have shown that the Gag portion of v-ErbA mediates CRM1-dependent nuclear export and that deletion of the Gag sequence results in a more nuclear localization of the protein (DeLong et al., 2004). Here, we show that deletion of the v-ErbA Gag sequence results in aggresome formation in only ~1% of cells, although this substantial decrease in aggresome formation is dependent in part on the shift of ΔGag-v-ErbA to a more nuclear distribution. The functional role of Gag-mediated nuclear export of v-ErbA remains to be determined, but the results in this present study support the hypothesis that it could be a remnant behavior of viral assembly. The N-terminal region of AEV Gag may promote enhanced targeting of v-ErbA to cytoplasmic aggresomes. Specific aggresome targeting sequences have been reported in the literature for other proteins, such as synphilin 1 (Zaarur et al., 2008). In contrast, the majority of Rous sarcoma virus (RSV) Gag accumulates in large, round structures in the cytoplasm called C-terminal TSG101-induced cellular structures (TICS) (Johnson et al., 2005), which are similar, but not identical to, classic aggresomes, and do not colocalize with GFP-250.

3.3 Are aggresomes pathogenic or cytoprotective?

Dysregulation of quality control pathways for degradation of misfolded proteins has been implicated in numerous clinical diseases, including cystic fibrosis, neurodegenerative disorders and cancer (Heir et al., 2006; Iwata et al., 2005; Johnston et al., 1998; Kitami et al., 2006; Ma and Lindquist, 2001; Mittal et al., 2007; Muchowski, 2002; Olzmann and Chin, 2008; Opazo et al., 2008; Riley et al., 2002; Ross and Poirier, 2004; Saliba et al., 2002; Sha et al., 2009; Shimohata et al., 2002; Simms-Waldrip et al., 2008; Taylor et al., 2003; Waelter et al., 2001; Winton et al., 2008). Despite their prevalence in disease and their being a focus of many detailed studies, there are a number of remaining questions about aggresome formation and the functional significance of these structures.

Recently, it has been suggested that there are multiple compartments in addition to the classic aggresome to which misfolded proteins can be trafficked. One report suggests that misfolded proteins partition between two distinct quality control compartments: juxtanuclear quality control (JUNQ) and insoluble protein deposit (IPOD) (Kaganovich et al., 2008). Aggresomes and another quality control compartment, the ER-associated compartment (ERAC), have features in common with the JUNQ compartment, but are proposed to differ in their architecture. In addition, nuclear aggresome-like structures form in cell lines

transfected with vectors expressing the puromycin resistance gene, suggesting that these vectors elicit an unexpected misfolded protein response (Moran et al., 2009). It is not yet clear whether all these inclusions represent related compartments or whether they have specialized functions (Bagola and Sommer, 2008).

Regardless of whether inclusions represent classical aggresomes or some related compartment, due to the high degree of correlation between aggregate formation and pathogenesis, it has been questioned whether these inclusions contribute to pathogenesis, or whether the underlying cause of pathogenicity is the lack of a functional protein. Aggresomes thus have been proposed to be cytoprotective, in part because they sequester deleterious, aggregrated proteins and may facilitate their elimination by autophagy (Green and Kroemer, 2009; Olzmann and Chin, 2008; Zhou et al., 2009). A number of studies have shown that reduced cytotoxicity is associated with aggresome formation (Arrasate et al., 2004; Fortun et al., 2003; Iwata et al., 2005; Tanaka et al., 2004; Taylor et al., 2003). Even more recently, aggresome formation has been implicated as a physiologic mechanism to regulate certain native cellular proteins; for example, cellular inactivation of inducible nitric oxide synthase (iNOS) (Pandit et al., 2009; Sha et al., 2009).

Whether the association of v-ErbA with aggresomes is pathogenic, cytoprotective, or physiologic remains an enigma. If viewed as a mechanism of sequestering excess v-ErbA for proteasome-mediated degradation or autophagy, then formation of the aggresome would appear to be cytoprotective. If one only considered the nuclear function of v-ErbA, then aggresome formation could be proposed to protect cells from the dominant negative activity of v-ErbA on nuclear receptors in the nucleus. However, when the full spectrum of v-ErbA subcellular trafficking is taken into account, then aggresome formation would appear to have pathogenic consequences. It is well documented that v-ErbA can sequester TRα1 and the retinoid X receptor in cytoplasmic foci, preventing these nuclear receptors from regulating transcription of target genes and, thereby, increasing dominant negative activity (Bonamy and Allison, 2006; Bonamy et al., 2005, and the present study). It is of interest to note that other dominant negative variants of TR form cytoplasmic foci (Bunn et al., 2001; Lee and Mahdavi, 1993), suggesting that this altered distribution pattern plays a role in their repressive action. Furthermore, specific mutations of TR genes are closely associated with endocrine disorders as well as several types of human cancers (Chan and Privalsky, 2009; Chan and Privalsky, 2010), and functional loss of both TRα1 and TRβ promotes tumor development in a mouse model of thyroid cancer (Zhu et al., 2010). Considered together, it is tempting to speculate that mislocalization of these variants is integral to pathogenesis. Comprehensive analysis of the effects of known mutations in TR on intracellular trafficking should help to clarify the relative contribution of receptor mislocalization to dominant negative activity and pathogenesis.

Compartmentalization also plays an important role in dominant negative activity of several other proteins and is central to disease pathogenesis. For example, in autosomal dominant retinitis pigmentosa, aggresomes containing mutant rhodopsin have been shown to recruit the normal wild-type protein (Saliba et al., 2002). In addition mutant ELOV4 (Elongation of very long-chain fatty acids-4) protein exerts a dominant negative effect, forming aggregates with the wild-type protein and contributing to pathogenesis in autosomal dominant

Stargardt-like macular dystrophy (Vasireddy et al., 2005). Similarly, the adenoviral E1B-55K oncoprotein forms aggresomes that sequester sequence-specific single-stranded DNA-binding protein 2, p53, and the MRE11-RAD50-NBS1 complex (MRN) (Fleisig et al., 2007; Liu et al., 2005). This stimulates the rate of proteasome-mediated degradation of MRN, thereby contributing to the protection of viral DNA from MRN activity.

In summary, the results presented here provide novel insight into the subcellular trafficking and function of the oncoprotein v-ErbA. In addition to rapid nucleocytoplasmic shuttling, the oncoprotein is trafficked along the aggresomal pathway, forming aggresomes that sequester and mislocalize nuclear receptors. In addition to mislocalizing nuclear receptors (Bonamy et al., 2005), v-ErbA also forms complexes with Smad4 and disrupts Smad4 nuclear localization, which is necessary for a functional TGF-β pathway (Erickson and Liu, 2009). Whether Smad4 is sequestered in aggresomes will be of interest to investigate. Finally, our studies contribute to a general understanding of the aggresome and its role in pathogenesis, cytoprotection, and protein turn-over. Although understanding of the precise molecular mechanisms remains limited, and many questions remain as to the underlying cellular mechanisms and means of regulation, the aggresome trafficking pathway is considered a viable target for treatment of neurodegenerative diseases (Olzmann and Chin, 2008; Zhang et al., 2007) and cancer (Rodriguez-Gonzalez et al., 2008). A complex model of v-ErbA function across three separate cellular compartments is emerging; these results add to the depth of understanding of v-ErbA activity and highlight the importance of altered subcellular trafficking for oncogenic disruption of gene regulation.

4. Materials and Methods

4.1 Plasmids

The GFP-250 and GFP170* expression vectors were a generous gift from Elizabeth Sztul (University of Alabama) (Fu et al., 2005; Garcia-Mata et al., 1999). The aggresomal marker GFP-250 is composed of GFP fused at its C-terminus to the first 250 amino acids of p115, a protein involved in the transport of cargo from the endoplasmic reticulum to the Golgi (Nelson et al., 1998). GFP170* is composed of GFP fused to amino acids 566–1375 of the Golgi Complex Protein (GCP)-170, which is also known as golgin-160 (Fu et al., 2005; Hicks and Machamer, 2002). GFP and DsRed2-tagged v-ErbA, GFP-TRα1, GFP-Δ Gag-v-ErbA, and YFP-Gag (1–70) expression vectors have been previously described (Bonamy et al., 2005; Bunn et al., 2001; DeLong et al., 2004). Myc-tagged p50/dynamitin (pCMV H50myc) was a generous gift from Richard Vallee (Columbia University). The Dendra2-v-ErbA expression vector was prepared by subcloning the v-ErbA coding region from GFP-v-ErbA into Dendra2-C (Evrogen). The mCherry-TRα1 expression vector was prepared by subcloning the TRα1 coding region from GFP-TRα1 into mCherry-C1 (Clontech). The GFP-GST-GFP expression vector consists of the glutathione-S-transferase (GST) and GFP coding regions subcloned in-frame into EGFP-C1 (Clontech). The expression vector for GFP-tagged glucocorticoid receptor (GFP-GR) was obtained from Bryce Paschal (University of Virginia) (Black et al., 2001).

4.2 Cell culture, transfections, and drug treatments

HeLa cells (human cervix epithelioid carcinoma; ATCC CCL-2) were grown and maintained at 37°C and 5% CO_2 in Minimum Es sential Medium (Gibco), supplemented with 10% fetal bovine serum (Invitrogen) and intermittently supplemented with 100 U/mL penicillin and 100 μg/mL streptomycin. HD3 cells (chicken erythroblasts transformed with AEV) were a generous gift from Xuedong Liu (University of Colorado-Boulder). HD3 cells were maintained in DMEM (Gibco) supplemented with 8% fetal bovine serum and 2% chicken serum (Invitrogen; heat inactivated for 1 h at 56°C).

For transient transfection assays, 1–3 × 10^5 HeLa cells per well were added to each well of a 6-well plate with glass coverslips (Fisher) and incubated at 37°C for approximately 24 h. Various combinations of plasmid expression vectors were introduced using either Lipofectamine or Lipofectamine 2000 (Invitrogen) according to the manufacturer's recommendations. Cells were fixed 24–48 h post-transfection and analyzed by fluorescence microscopy. In some experiments, cells were treated with 2–4 nM leptomycin B (Sigma) or vehicle (methanol) for 1–5 h, 100 nM 3,3′,5-triiodo-L-thyronine (T_3) (Sigma), the proteasome-inhibiting drug MG132 (10 μg/ml, Sigma; or 10 μM, Calbiochem), the microtubule-disrupting drug nocodazole (10 μg/ml, Sigma), or an equivalent volume of vehicle (DMSO) for 12–20 hr post-transfection.

4.3 Fixation, immunofluorescence, and organelle staining

Approximately 24–48 hours after transfection, cells were fixed in 3.7% formaldehyde and permeabilized with 0.2% Triton-X-100. Antibodies used were as follows: anti-v-ErbA/c-ErbA, 1:100 (FL-408, Santa Cruz Biotechnologies); Cy3-conjugated anti-vimentin, 1:200 (Sigma); anti-c-myc, 1:500 (Clontech); anti-20S proteasome 'core' subunits, 1:500 (BioMol); anti-HDAC6, 1:100 (Santa Cruz Biotechnologies); anti-ubiquitin, 1:100 (Calbiochem); anti-Hsp70 1:50 (Stressgen); Cy3-goat anti-mouse or Cy3-goat anti-rabbit, 1:500 (Zymed Laboratories); and FITC-conjugated anti-β-tubulin, 1/10 (Sigma). To visualize mitochondria, cells were treated with 10 nM MitoTracker Red (Molecular Probes) approximately 48 h post-transfection. Upon addition of MitoTracker Red, cells were incubated at 37°C for 30 min. After processing, coverslips were mounted onto microscope slides in Fluoro-Gel II (Electron Microscopy Sciences) containing the DNA counter stain DAPI (4, 6-diamino-2-phenylindole).

4.4 Cell scoring and statistical analysis

For some experiments, prepared slides were analyzed with an Olympus fluorescence microscope. Cells were photographed with a Cooke SensiCamQE digital camera. IP Lab software and Adobe Photoshop CS were used to pseudocolor, and layer the captured images. For other experiments, images were collected from an inverted Nikon ECLIPSE TE 2000-E fluorescence microscope (Sigma, Melville, NY). A Nikon Ultraviolet Excitation: UV-2E/C filter block for DAPI visualization and a Blue Excitation: B-2E/C filter block for G3BP-GFP visualization were used with a Nikon Plan Apo 60x objective. A CoolSNAP HQ_2 CCD camera (Photometrics) and NIS-Elements AR software (Nikon) were used for image acquisition and primary image processing.

At least 2–3 replicate transfections were performed, with a minimum of 100 cells scored per replicate. Results were tested for statistical significance using SPSS (v. 16). Data were analyzed for frequency distribution using a Chi-Square test; a p-value of 0.001 or less was considered significant.

4.5 Immunoblotting

HeLa cells were seeded onto 100 mm plates (7×10^5 cells per plate) in MEM supplemented with charcoal-dextran stripped fetal bovine serum (Hyclone). Sixteen hours post-transfection, cells were treated with vehicle (DMSO), T_3 (100 nM, Sigma), or MG132 (10 μM, Calbiochem) for 16.5 hours. Subsequently, whole cell lysates were prepared using the Active Motif Nuclear Extract Kit, according to the manufacturer's instructions. For v-ErbA, both the supernatant and pellet fractions from each lysis were analyzed by SDS-PAGE; similar amounts of v-ErbA were distributed between the insoluble versus soluble fraction. The protein concentration was determined by spectrophotometry. Forty μg of whole cell extract per treatment were resolved by 8% SDS-PAGE and transferred to a PVDF membrane (GE Healthcare) by semi-dry electroblotting for immunoblot analysis with anti-GFP (1:200) (Santa Cruz Biotechnology) and anti-β-tubulin (1:200) (Santa Cruz Biotechnology) antibodies, followed by chemilumiscent detection using ECL Plus. Protein size was monitored using Pre-Stained Kaleidoscope Protein Standards (Bio-Rad).

4.6 Live cell imaging

After transfection, cells were used for microscopy within 48 h. Prior to mounting in an enclosed perfusion chamber (Bioptechs, Butler, PA), coverslips were incubated in 2 ml complete media containing 2–4 nM leptomycin B (LMB) (Sigma) or vehicle (0.1% methanol) for 30 min. Coverslips were then washed with 2 ml Dulbecco's phosphate buffered saline (D-PBS) and mounted. For the duration of each experiment, cells were incubated in MEMα (without phenol red) containing 2–4 nM LMB or vehicle (0.1% methanol). All life cell imaging was performed using the inverted Nikon ECLIPSE TE 2000-E fluorescence microscope.

Supplementary Material

Refer to Web version on PubMed Central for supplementary material.

Acknowledgments

We thank Drs. Elizabeth Sztul (University of Alabama) and Richard Vallee (Columbia University) for their generous gifts of plasmid expression vectors used in this study, Xuedong Liu (University of Colorado-Boulder) for the generous gift of the HD3 cell line, and Elizabeth A. Honenberger for pilot studies using p50/dynamitin. This work was supported in part by National Science Foundation Grant MCB0646506 to L.A.A., and by a Howard Hughes Medical Research Institute grant through the Undergraduate Science Biological Sciences Education Program to the College of William & Mary.

Abbreviations

TRα1	thyroid hormone receptor α1
T_3	thyroid hormone

AEV	avian erythroblastosis virus
TGF-β	transforming growth factor-β
LMB	leptomycin B
MTOC	microtubule organizing center
HDAC6	histone deacetylase 6
CFTR	cystic fibrosis transmembrane conductance regulator

References

Aranda A, Martínez-Iglesias O, Ruiz-Llorente L, García-Carpizo V, Zambrano A. Thyroid receptor: roles in cancer. Trends Endocrinol Metab. 2010; 20:318–324. [PubMed: 19716314]

Ardley HC, Scott GB, Rose SA, Tan NG, Robinson PA. UCH-L1 aggresome formation in response to proteasome impairment indicates a role in inclusion formation in Parkinson's disease. J Neurochem. 2004; 90:379–391. [PubMed: 15228595]

Arnaud F, Murcia PR, Palmarini M. Mechanisms of late restriction induced by an endogenous retrovirus. J Virol. 2007; 81:11441–11451. [PubMed: 17699582]

Arrasate M, Mitra S, Schweitzer ES, Segal MR, Finkbeiner S. Inclusion body formation reduces levels of mutant huntingtin and the risk of neuronal death. Nature. 2004; 431:805–810. [PubMed: 15483602]

Bagola K, Sommer T. Protein quality control: on IPODs and other JUNQ. Curr Biol. 2008; 18:R1019–1021. [PubMed: 19000801]

Bauer NG, Richter-Landsberg C. The dynamic instability of microtubules is required for aggresome formation in oligodendroglial cells after proteolytic stress. J Mol Neurosci. 2006; 29:153–168. [PubMed: 16954605]

Bercovich B, Stancovski I, Mayer A, Blumenfeld N, Laszlo A, Schwartz AL, Ciechanover A. Ubiquitin-dependent degradation of certain protein substrates in vitro requires the molecular chaperone Hsc70. J Biol Chem. 1997; 272:9002–9010. [PubMed: 9083024]

Beug H, Bauer A, Dolznig H, von Lindern M, Lobmayer L, Mellitzer G, Steinlein P, Wessely O, Mullner E. Avian erythropoiesis and erythroleukemia: towards understanding the role of the biomolecules involved. Biochim Biophys Acta. 1996; 1288:M35–47. [PubMed: 9011180]

Black BE, Holaska JM, Rastinejad F, Paschal BM. DNA binding domains in diverse nuclear receptors function as nuclear export signals. Curr Biol. 2001; 11:1749–1758. [PubMed: 11719216]

Bonamy GM, Allison LA. Oncogenic conversion of the thyroid hormone receptor by altered nuclear transport. Nucl Recept Signal. 2006; 4:e008. [PubMed: 16741566]

Bonamy GM, Guiochon-Mantel A, Allison LA. Cancer promoted by the oncoprotein v-ErbA may be due to subcellular mislocalization of nuclear receptors. Mol Endocrinol. 2005; 19:1213–1230. [PubMed: 15650025]

Boyault C, Zhang Y, Fritah S, Caron C, Gilquin B, Kwon SH, Garrido C, Yao TP, Vourc'h C, Matthias P, Khochbin S. HDAC6 controls major cell response pathways to cytotoxic accumulation of protein aggregates. Genes Dev. 2007; 21:2172–2181. [PubMed: 17785525]

Bresson C, Keime C, Faure C, Letrillard Y, Barbado M, Sanfilippo S, Benhra N, Gandrillon O, Gonin-Giraud S. Large-scale analysis by SAGE reveals new mechanisms of v-erbA oncogene action. BMC Genomics. 2007; 8:390. [PubMed: 17961265]

Bunn CF, Neidig JA, Freidinger KE, Stankiewicz TA, Weaver BS, McGrew J, Allison LA. Nucleocytoplasmic shuttling of the thyroid hormone receptor alpha. Mol Endocrinol. 2001; 15:512–533. [PubMed: 11266504]

Cereghetti GM, Scorrano L. The many shapes of mitochondrial death. Oncogene. 2006; 25:4717–4724. [PubMed: 16892085]

Chan IH, Privalsky ML. Thyroid hormone receptor mutants implicated in human hepatocellular carcinoma display an altered target gene repertoire. Oncogene. 2009; 28:4162–4174. [PubMed: 19749797]

Chan IH, Privalsky ML. A conserved lysine in the thyroid hormone receptor-alpha1 DNA-binding domain, mutated in hepatocellular carcinoma, serves as a sensor for transcriptional regulation. Mol Cancer Res. 2010; 8:15–23. [PubMed: 20053725]

Dace A, Zhao L, Park KS, Furuno T, Takamura N, Nakanishi M, West BL, Hanover JA, Cheng S. Hormone binding induces rapid proteasome-mediated degradation of thyroid hormone receptors. Proc Natl Acad Sci U S A. 2000; 97:8985–8990. [PubMed: 10908671]

Debure L, Vayssiere JL, Rincheval V, Loison F, Le Drean Y, Michel D. Intracellular clusterin causes juxtanuclear aggregate formation and mitochondrial alteration. J Cell Sci. 2003; 116:3109–3121. [PubMed: 12799419]

DeLong LJ, Bonamy GM, Fink EN, Allison LA. Nuclear export of the oncoprotein v-ErbA is mediated by acquisition of a viral nuclear export sequence. J Biol Chem. 2004; 279:15356–15367. [PubMed: 14729678]

Diaz-Griffero F, Li X, Javanbakht H, Song B, Welikala S, Stremlau M, Sodroski J. Rapid turnover and polyubiquitylation of the retroviral restriction factor TRIM5. Virology. 2006; 349:300–315. [PubMed: 16472833]

Dul JL, Davis DP, Williamson EK, Stevens FJ, Argon Y. Hsp70 and antifibrillogenic peptides promote degradation and inhibit intracellular aggregation of amyloidogenic light chains. J Cell Biol. 2001; 152:705–716. [PubMed: 11266462]

Erickson RA, Liu X. Association of v-ErbA with Smad4 disrupts TGF-beta signaling. Mol Biol Cell. 2009; 20:1509–1519. [PubMed: 19144825]

Fleisig HB, Orazio NI, Liang H, Tyler AF, Adams HP, Weitzman MD, Nagarajan L. Adenoviral E1B55K oncoprotein sequesters candidate leukemia suppressor sequence-specific single-stranded DNA-binding protein 2 into aggresomes. Oncogene. 2007; 26:4797–4805. [PubMed: 17311003]

Fortun J, Dunn WA Jr, Joy S, Li J, Notterpek L. Emerging role for autophagy in the removal of aggresomes in Schwann cells. J Neurosci. 2003; 23:10672–10680. [PubMed: 14627652]

Fu L, Gao YS, Tousson A, Shah A, Chen TL, Vertel BM, Sztul E. Nuclear aggresomes form by fusion of PML-associated aggregates. Mol Biol Cell. 2005; 16:4905–4917. [PubMed: 16055507]

Garcia-Mata R, Bebok Z, Sorscher EJ, Sztul ES. Characterization and dynamics of aggresome formation by a cytosolic GFP-chimera. J Cell Biol. 1999; 146:1239–1254. [PubMed: 10491388]

Garcia-Mata R, Gao YS, Sztul E. Hassles with taking out the garbage: aggravating aggresomes. Traffic. 2002; 3:388–396. [PubMed: 12010457]

Gonin-Giraud S, Bresson-Mazet C, Gandrillon O. Involvement of the TGF-beta and mTOR/p70S6Kinase pathways in the transformation process induced by v-ErbA. Leuk Res. 2008; 32:1878–1888. [PubMed: 18573525]

Green DR, Kroemer G. Cytoplasmic functions of the tumour suppressor p53. Nature. 2009; 458:1127–1130. [PubMed: 19407794]

Heath CM, Windsor M, Wileman T. Aggresomes resemble sites specialized for virus assembly. J Cell Biol. 2001; 153:449–455. [PubMed: 11331297]

Heir R, Ablasou C, Dumontier E, Elliott M, Fagotto-Kaufmann C, Bedford FK. The UBL domain of PLIC-1 regulates aggresome formation. EMBO Rep. 2006; 7:1252–1258. [PubMed: 17082820]

Hicks SW, Machamer CE. The NH2-terminal domain of Golgin-160 contains both Golgi and nuclear targeting information. J Biol Chem. 2002; 277:35833–35839. [PubMed: 12130652]

Iwata A, Riley BE, Johnston JA, Kopito RR. HDAC6 and microtubules are required for autophagic degradation of aggregated huntingtin. J Biol Chem. 2005; 280:40282–40292. [PubMed: 16192271]

Johnson MC, Spidel JL, Ako-Adjei D, Wills JW, Vogt VM. The C-terminal half of TSG101 blocks Rous sarcoma virus budding and sequesters Gag into unique nonendosomal structures. J Virol. 2005; 79:3775–3786. [PubMed: 15731271]

Johnston JA, Dalton MJ, Gurney ME, Kopito RR. Formation of high molecular weight complexes of mutant Cu, Zn-superoxide dismutase in a mouse model for familial amyotrophic lateral sclerosis. Proc Natl Acad Sci U S A. 2000; 97:12571–12576. [PubMed: 11050163]

Johnston JA, Illing ME, Kopito RR. Cytoplasmic dynein/dynactin mediates the assembly of aggresomes. Cell Motil Cytoskeleton. 2002; 53:26–38. [PubMed: 12211113]

Johnston JA, Ward CL, Kopito RR. Aggresomes: a cellular response to misfolded proteins. J Cell Biol. 1998; 143:1883–1898. [PubMed: 9864362]

Kabore AF, Wang WJ, Russo SJ, Beers MF. Biosynthesis of surfactant protein C: characterization of aggresome formation by EGFP chimeras containing propeptide mutants lacking conserved cysteine residues. J Cell Sci. 2001; 114:293–302. [PubMed: 11148131]

Kaganovich D, Kopito R, Frydman J. Misfolded proteins partition between two distinct quality control compartments. Nature. 2008; 454:1088–1095. [PubMed: 18756251]

Kawaguchi Y, Kovacs JJ, McLaurin A, Vance JM, Ito A, Yao TP. The deacetylase HDAC6 regulates aggresome formation and cell viability in response to misfolded protein stress. Cell. 2003; 115:727–738. [PubMed: 14675537]

Kenessey A, Ojamaa K. Ligand-mediated decrease of thyroid hormone receptor-alpha1 in cardiomyocytes by proteosome-dependent degradation and altered mRNA stability. Am J Physiol Heart Circ Physiol. 2005; 288:H813–821. [PubMed: 15498821]

Kitami MI, Kitami T, Nagahama M, Tagaya M, Hori S, Kakizuka A, Mizuno Y, Hattori N. Dominant-negative effect of mutant valosin-containing protein in aggresome formation. FEBS Lett. 2006; 580:474–478. [PubMed: 16386250]

Kopito RR. Aggresomes, inclusion bodies and protein aggregation. Trends Cell Biol. 2000; 10:524–530. [PubMed: 11121744]

Kuemmerle S, Gutekunst CA, Klein AM, Li XJ, Li SH, Beal MF, Hersch SM, Ferrante RJ. Huntington aggregates may not predict neuronal death in Huntington's disease. Ann Neurol. 1999; 46:842–849. [PubMed: 10589536]

Kutay U, Guttinger S. Leucine-rich nuclear-export signals: born to be weak. Trends Cell Biol. 2005; 15:121–124. [PubMed: 15752974]

Lee DH, Goldberg AL. Proteasome inhibitors: valuable new tools for cell biologists. Trends Cell Biol. 1998; 8:397–403. [PubMed: 9789328]

Lee Y, Mahdavi V. The D domain of the thyroid hormone receptor alpha 1 specifies positive and negative transcriptional regulation functions. J Biol Chem. 1993; 268:2021–2028. [PubMed: 8420976]

Levine B, Kroemer G. Autophagy in the pathogenesis of disease. Cell. 2008; 132:27–42. [PubMed: 18191218]

Liu Y, Shevchenko A, Berk AJ. Adenovirus exploits the cellular aggresome response to accelerate inactivation of the MRN complex. J Virol. 2005; 79:14004–14016. [PubMed: 16254336]

Luduena RF, Roach MC. Tubulin sulfhydryl groups as probes and targets for antimitotic and antimicrotubule agents. Pharmacol Ther. 1991; 49:133–152. [PubMed: 1852786]

Ma J, Lindquist S. Wild-type PrP and a mutant associated with prion disease are subject to retrograde transport and proteasome degradation. Proc Natl Acad Sci U S A. 2001; 98:14955–14960. [PubMed: 11742063]

Melkonian KA, Maier KC, Godfrey JE, Rodgers M, Schroer TA. Mechanism of dynamitin-mediated disruption of dynactin. J Biol Chem. 2007; 282:19355–19364. [PubMed: 17449914]

Mignot C, Delarasse C, Escaich S, Della Gaspera B, Noe E, Colucci-Guyon E, Babinet C, Pekny M, Vicart P, Boespflug-Tanguy O, et al. Dynamics of mutated GFAP aggregates revealed by real-time imaging of an astrocyte model of Alexander disease. Exp Cell Res. 2007; 313:2766–2779. [PubMed: 17604020]

Mittal S, Dubey D, Yamakawa K, Ganesh S. Lafora disease proteins malin and laforin are recruited to aggresomes in response to proteasomal impairment. Hum Mol Genet. 2007; 16:753–762. [PubMed: 17337485]

Mizushima N, Levine B, Cuervo AM, Klionsky DJ. Autophagy fights disease through cellular self-digestion. Nature. 2008; 451:1069–1075. [PubMed: 18305538]

Moran DM, Shen H, Maki CG. Puromycin-based vectors promote a ROS-dependent recruitment of PML to nuclear inclusions enriched with HSP70 and Proteasomes. BMC Cell Biol. 2009; 10:32. [PubMed: 19409099]

Morimoto RI. Proteotoxic stress and inducible chaperone networks in neurodegenerative disease and aging. Genes Dev. 2008; 22:1427–1438. [PubMed: 18519635]

Mortimore GE, Miotto G, Venerando R, Kadowaki M. Autophagy. Subcell Biochem. 1996; 27:93–135. [PubMed: 8993159]

Muchowski PJ. Protein misfolding, amyloid formation, and neurodegeneration: a critical role for molecular chaperones? Neuron. 2002; 35:9–12. [PubMed: 12123602]

Muqit MM, Abou-Sleiman PM, Saurin AT, Harvey K, Gandhi S, Deas E, Eaton S, Payne Smith MD, Venner K, Matilla A, et al. Altered cleavage and localization of PINK1 to aggresomes in the presence of proteasomal stress. J Neurochem. 2006; 98:156–169. [PubMed: 16805805]

Nelson DS, Alvarez C, Gao YS, Garcia-Mata R, Fialkowski E, Sztul E. The membrane transport factor TAP/p115 cycles between the Golgi and earlier secretory compartments and contains distinct domains required for its localization and function. J Cell Biol. 1998; 143:319–331. [PubMed: 9786945]

Nozawa N, Yamauchi Y, Ohtsuka K, Kawaguchi Y, Nishiyama Y. Formation of aggresome-like structures in herpes simplex virus type 2-infected cells and a potential role in virus assembly. Exp Cell Res. 2004; 299:486–497. [PubMed: 15350546]

Olzmann JA, Chin LS. Parkin-mediated K63-linked polyubiquitination: a signal for targeting misfolded proteins to the aggresome-autophagy pathway. Autophagy. 2008; 4:85–87. [PubMed: 17957134]

Opazo F, Krenz A, Heermann S, Schulz JB, Falkenburger BH. Accumulation and clearance of alpha-synuclein aggregates demonstrated by time-lapse imaging. J Neurochem. 2008; 106:529–540. [PubMed: 18410502]

Pandit L, Kolodziejska KE, Zeng S, Eissa NT. The physiologic aggresome mediates cellular inactivation of iNOS. Proc Natl Acad Sci U S A. 2009; 106:1211–1215. [PubMed: 19139419]

Pankiv S, Clausen TH, Lamark T, Brech A, Bruun JA, Outzen H, Overvatn A, Bjorkoy G, Johansen T. p62/SQSTM1 binds directly to Atg8/LC3 to facilitate degradation of ubiquitinated protein aggregates by autophagy. J Biol Chem. 2007; 282:24131–24145. [PubMed: 17580304]

Prichard MN, Sztul E, Daily SL, Perry AL, Frederick SL, Gill RB, Hartline CB, Streblow DN, Varnum SM, Smith RD, Kern ER. Human cytomegalovirus UL97 kinase activity is required for the hyperphosphorylation of retinoblastoma protein and inhibits the formation of nuclear aggresomes. J Virol. 2008; 82:5054–5067. [PubMed: 18321963]

Privalsky ML. A subpopulation of the v-erb A oncogene protein, a derivative of a thyroid hormone receptor, associates with heat shock protein 90. J Biol Chem. 1991; 266:1456–1462. [PubMed: 1671036]

Riley NE, Li J, Worrall S, Rothnagel JA, Swagell C, van Leeuwen FW, French SW. The Mallory body as an aggresome: in vitro studies. Exp Mol Pathol. 2002; 72:17–23. [PubMed: 11784119]

Rodriguez-Gonzalez A, Lin T, Ikeda AK, Simms-Waldrip T, Fu C, Sakamoto KM. Role of the aggresome pathway in cancer: targeting histone deacetylase 6-dependent protein degradation. Cancer Res. 2008; 68:2557–2560. [PubMed: 18413721]

Ross CA, Poirier MA. Protein aggregation and neurodegenerative disease. Nat Med. 2004; 10(Suppl):S10–17. [PubMed: 15272267]

Rubinsztein DC. The roles of intracellular protein-degradation pathways in neurodegeneration. Nature. 2006; 443:780–786. [PubMed: 17051204]

Saliba RS, Muñoz PM, Luthert PJ, Cheetham ME. The cellular fate of mutant rhodopsin: quality control, degradation and aggresome formation. J Cell Sci. 2002; 115:2907–2918. [PubMed: 12082151]

Sap J, Muñoz A, Damm K, Goldberg Y, Ghysdael J, Leutz A, Beug H, Vennström B. The c-erb-A protein is a high-affinity receptor for thyroid hormone. Nature. 1986; 324:635–640. [PubMed: 2879242]

Schroder M, Kaufman RJ. The mammalian unfolded protein response. Annu Rev Biochem. 2005; 74:739–789. [PubMed: 15952902]

Sha Y, Pandit L, Zeng S, Eissa NT. A critical role for CHIP in the aggresome pathway. Mol Cell Biol. 2009; 29:116–128. [PubMed: 18955503]

Shimohata T, Sato A, Burke JR, Strittmatter WJ, Tsuji S, Onodera O. Expanded polyglutamine stretches form an 'aggresome'. Neurosci Lett. 2002; 323:215–218. [PubMed: 11959423]

Simms-Waldrip T, Rodriguez-Gonzalez A, Lin T, Ikeda AK, Fu C, Sakamoto KM. The aggresome pathway as a target for therapy in hematologic malignancies. Mol Genet Metab. 2008; 94:283–286. [PubMed: 18472289]

Soo KY, Atkin JD, Horne MK, Nagley P. Recruitment of mitochondria into apoptotic signaling correlates with the presence of inclusions formed by amyotrophic lateral sclerosis-associated SOD1 mutations. J Neurochem. 2009; 108:578–590. [PubMed: 19046404]

Suzuki T. Explorative study on isoform-selective histone deacetylase inhibitors. Chem Pharm Bull (Tokyo). 2009; 57:897–906. [PubMed: 19721249]

Szebenyi G, Wigley WC, Hall B, Didier A, Yu M, Thomas P, Kramer H. Hook2 contributes to aggresome formation. BMC Cell Biol. 2007; 8:19. [PubMed: 17540036]

Tanaka M, Kim YM, Lee G, Junn E, Iwatsubo T, Mouradian MM. Aggresomes formed by alpha-synuclein and synphilin-1 are cytoprotective. J Biol Chem. 2004; 279:4625–4631. [PubMed: 14627698]

Taylor JP, Tanaka F, Robitschek J, Sandoval CM, Taye A, Markovic-Plese S, Fischbeck KH. Aggresomes protect cells by enhancing the degradation of toxic polyglutamine-containing protein. Hum Mol Genet. 2003; 12:749–757. [PubMed: 12651870]

Thormeyer D, Baniahmad A. The v-erbA oncogene (review). Int J Mol Med. 1999; 4:351–358. [PubMed: 10493974]

Vasireddy V, Vijayasarathy C, Huang J, Wang XF, Jablonski MM, Petty HR, Sieving PA, Ayyagari R. Stargardt-like macular dystrophy protein ELOVL4 exerts a dominant negative effect by recruiting wild-type protein into aggresomes. Mol Vis. 2005; 11:665–676. [PubMed: 16163264]

Vasquez RJ, Howell B, Yvon AM, Wadsworth P, Cassimeris L. Nanomolar concentrations of nocodazole alter microtubule dynamic instability in vivo and in vitro. Mol Biol Cell. 1997; 8:973–985. [PubMed: 9201709]

Ventura-Holman T, Mamoon A, Subauste JS. Modulation of expression of RA-regulated genes by the oncoprotein v-erbA. Gene. 2008; 425:23–27. [PubMed: 18775481]

Waelter S, Boeddrich A, Lurz R, Scherzinger E, Lueder G, Lehrach H, Wanker EE. Accumulation of mutant huntingtin fragments in aggresome-like inclusion bodies as a result of insufficient protein degradation. Mol Biol Cell. 2001; 12:1393–1407. [PubMed: 11359930]

Wigley WC, Fabunmi RP, Lee MG, Marino CR, Muallem S, DeMartino GN, Thomas PJ. Dynamic association of proteasomal machinery with the centrosome. J Cell Biol. 1999; 145:481–490. [PubMed: 10225950]

Wileman T. Aggresomes and autophagy generate sites for virus replication. Science. 2006; 312:875–878. [PubMed: 16690857]

Wileman T. Aggresomes and pericentriolar sites of virus assembly: cellular defense or viral design? Annu Rev Microbiol. 2007; 61:149–167. [PubMed: 17896875]

Winton MJ, Igaz LM, Wong MM, Kwong LK, Trojanowski JQ, Lee VM. Disturbance of nuclear and cytoplasmic TAR DNA-binding protein (TDP-43) induces disease-like redistribution, sequestration, and aggregate formation. J Biol Chem. 2008; 283:13302–13309. [PubMed: 18305110]

Wong ES, Tan JM, Soong WE, Hussein K, Nukina N, Dawson VL, Dawson TM, Cuervo AM, Lim KL. Autophagy-mediated clearance of aggresomes is not a universal phenomenon. Hum Mol Genet. 2008; 17:2570–2582. [PubMed: 18502787]

Zaarur N, Meriin AB, Gabai VL, Sherman MY. Triggering aggresome formation. Dissecting aggresome-targeting and aggregation signals in synphilin 1. J Biol Chem. 2008; 283:27575–27584. [PubMed: 18635553]

Zhang L, Yu J, Pan H, Hu P, Hao Y, Cai W, Zhu H, Yu AD, Xie X, Ma D, Yuan J. Small molecule regulators of autophagy identified by an image-based high-throughput screen. Proc Natl Acad Sci U S A. 2007; 104:19023–19028. [PubMed: 18024584]

Zhou X, Ikenoue T, Chen X, Li L, Inoki K, Guan KL. Rheb controls misfolded protein metabolism by inhibiting aggresome formation and autophagy. Proc Natl Acad Sci U S A. 2009; 106:8923–8928. [PubMed: 19458266]

Zhu XG, Zhao L, Willingham MC, Cheng SY. Thyroid hormone receptors are tumor suppressors in a mouse model of metastatic follicular thyroid carcinoma. Oncogene. 2010; 29:1909–1919. [PubMed: 20062085]

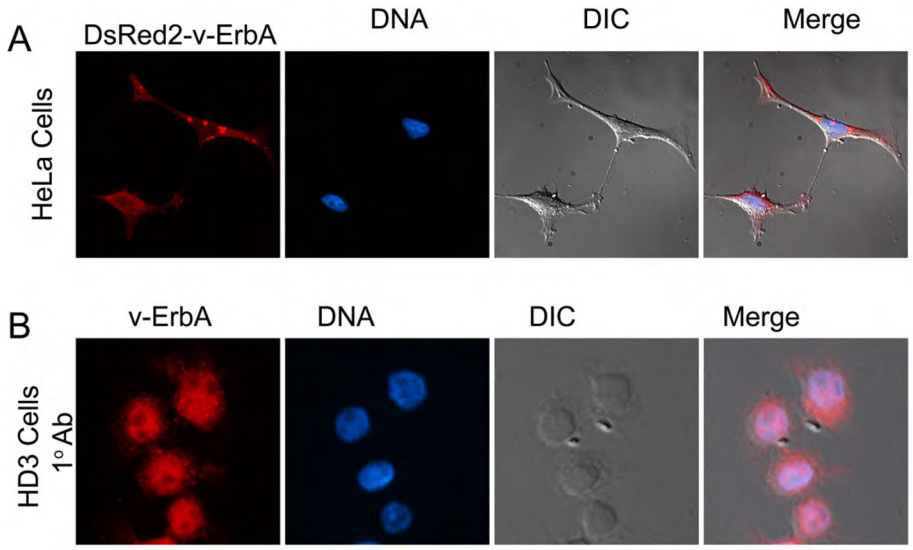

Fig. 1.

A subpopulation of the oncoprotein v-ErbA localizes to punctate foci in erythroblasts transformed with AEV. (A) The distribution of v-ErbA in transfected HeLa cells ranges from whole cell (with a nuclear subpopulation) to a mainly cytoplasmic distribution, localized in punctate, perinuclear foci. HeLa cells were transfected with DsRed2-v-ErbA expression vectors. 24h post-transfection, cells were fixed and analyzed by fluorescence and differential interference contrast (DIC) microscopy. Nuclei were stained for DNA with DAPI (blue). (B) Native, virally-expressed v-ErbA forms cytoplasmic foci in chicken erythroblasts transformed with AEV (HD3 cells). Native v-ErbA was visualized in HD3 cells by immunostaining (red).

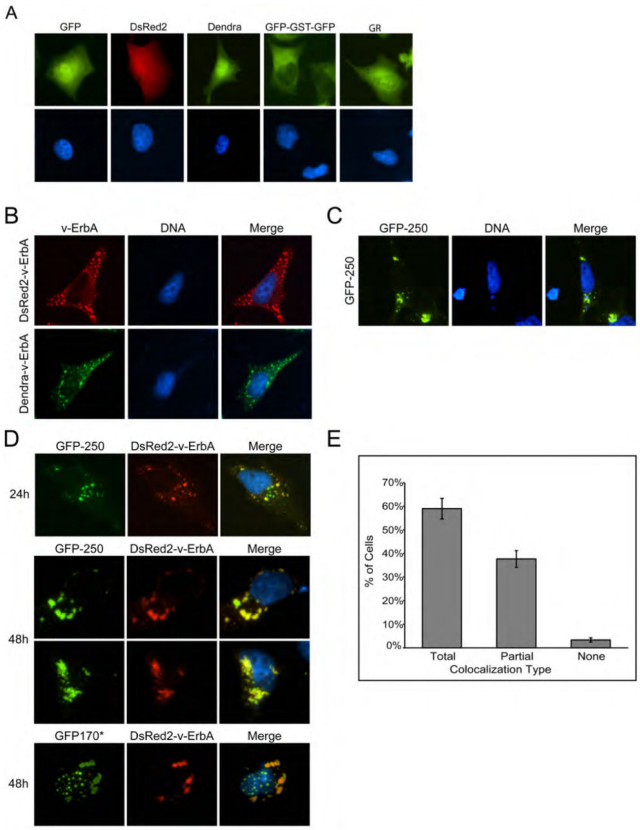

Fig. 2.

The oncoprotein v-ErbA colocalizes with aggresomal markers. (A) Fluorescent proteins alone and control GFP-tagged fusion proteins do not localize to cytoplasmic foci. HeLa cells were transfected with expression vectors for GFP, DsRed2, Dendra, GFP-GST-GFP, or GFP-glucocorticoid receptor (GFP-GR). Twenty-four hours post-transfection, cells were fixed and analyzed by fluorescence microscopy. Nuclei were stained for DNA with DAPI (blue). (B) A subpopulation of DsRed2-tagged and Dendra2 (monomeric fluorescent protein)-tagged v-ErbA localizes to cytoplasmic foci. HeLa cells were cotransfected with either DsRed2-tagged or Dendra2-tagged v-ErbA expression vectors and processed as described in (A). (C) Localization of the aggresomal marker GFP-250 24 h post-transfection. (D) Colocalization of the aggresomal markers GFP-250, GFP170*, and DsRed2-v-ErbA. HeLa cells were cotransfected with either GFP-250 or GFP170*, and DsRed2-v-ErbA expression vectors. Either 24 h or 48 h post-transfection, as indicated, cells were fixed and analyzed by fluorescence microscopy. In the merged images, yellow indicates colocalization between either GFP-250 or GFP170* and DsRed2-v-ErbA. (E) Bar graph summarizing colocalization data for GFP-250 and DsRed2-v-ErbA. Forty-eight hours post-transfection, DsRed2-v-ErbA and GFP-250 completely colocalized (Total) in 59 ± 4% of cells and partially colocalized (Partial) in 38 ± 4% of cells (n=3 replicate transfections, 313 cells scored). Error bars indicate ±SEM.

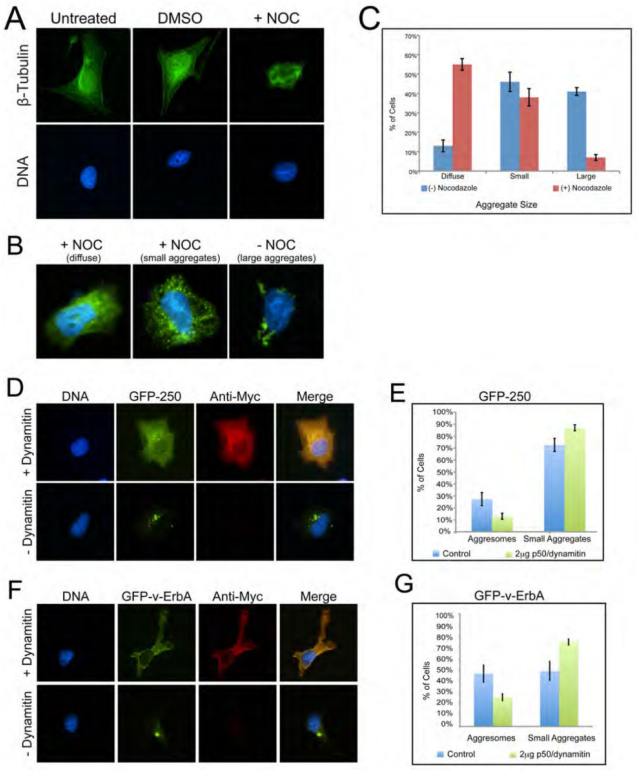

Fig. 3.

Formation of v-ErbA foci is microtubule-and dynein-dependent. (A) Treatment with nocodozole disrupts microtubules. HeLa cells were either left untreated, treated with DMSO (vehicle control), or treated with nocodozole (+NOC) for 20 h. Microtubules were visualized by immunostaining with Cy3-tagged anti-β-tubulin (red). Nuclei were stained for DNA with DAPI (blue) (B) Microtubule disruption prevents the formation of coalesced v-ErbA foci. HeLa cells were transfected with an expression vector for GFP-v-ErbA, and 16 h post-transfection were treated with nocodazole for 20 h. +NOC (diffuse), nocodazole-treated cell forming diffuse aggregates; +NOC (small aggregates), nocodazole-treated cell forming small aggregates, uniform in size; −NOC, untreated cell forming large juxtanuclear foci. (C) Bar graph summarizing the effect of nocodozole on v-ErbA foci size. Upon nocodazole treatment, there was a significant shift ($p < 0.001$) in frequency distribution from larger foci to smaller, more diffuse foci. Error bars indicate ±SEM (n=2 replicates, 200 cells scored). (D–G) Overexpression of p50/dynamitin disrupts aggresome formation. (D) HeLa cells were transfected with GFP-250 expression vector alone (−Dynamitin) or together with Myc-tagged p50/dynamitin expression vector (+Dynamitin). After 24–48 h, cells were fixed, immunostained with anti-Myc antibodies (red) and analyzed by fluorescence microscopy. Blue, nucleistained for DNA with DAPI. In the absence of p50/dynamitin, GFP-250 formed mature aggresomes. In the presence of p50 dynamitin, smaller aggregates formed. (E) Bar graph summarizing the effect of p50/dyamitin on GFP-250 aggresome formation. Error bars indicate ±SEM (n=3 replicates, 100 cells scored per replicate). (F) HeLa cells were transfected with GFP-v-ErbA expression vector alone (−Dynamitin) or together with Myc-tagged p50 dynamitin expression vector (+Dynamitin). After 24–48 h, cells were fixed and

analyzed by fluorescence microscopy. In the absence of p50/dynamitin GFP-v-ErbA formed mature aggresomes. In the presence of p50/dynamitin, smaller aggregates formed. (G) Bar graph summarizing the effect of p50/dynamitin on GFP-v-ErbA aggresome formation. Error bars indicate ±SEM (n=3 replicates, 100 cells scored per replicate).

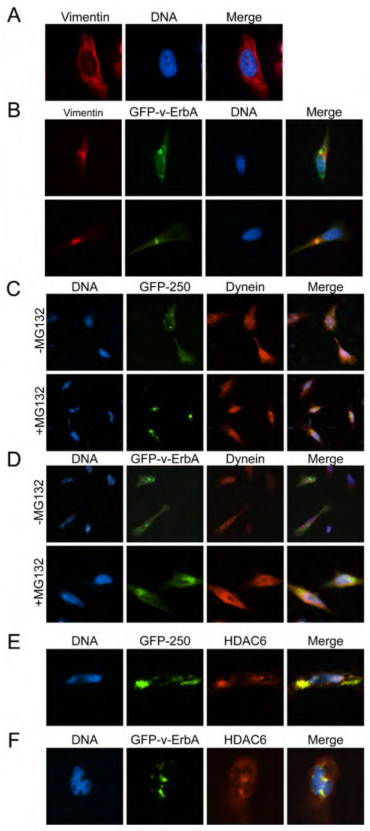

Fig. 4.

v-ErbA foci disrupt vimentin intermediate filaments and colocalize with HDAC6. (A) In untransfected cells, the vimentin distribution pattern was filamentous and dispersed throughout the cell. After fixation, HeLa cells were stained with a Cy3-conjugated antibody against vimentin (red); nuclei were stained for DNA with DAPI (blue). (B) v-ErbA foci cause a disruption of vimentin filaments. HeLa cells transfected with GFP-v-ErbA were immunostained for vimentin 48 h post-transfection (n=3, > 300 cells scored). Green, distribution of GFP-v-ErbA; Red, distribution of Cy3-conjugated antibody against vimentin; Merge, layered image of GFP-v-ErbA and Cy3-vimentin; Blue, nuclei stained for DNA with DAPI. Cells transfected with GFP-v-ErbA showed a reorganization and collapse of vimentin around the area of aggregated protein. (C, D) GFP-250 and GFP-v-ErbA aggresomes are not enriched for dynein. HeLa cells were transfected with either GFP-250 (C) or GFP-v-ErbA (D), as indicated, and 16 h post-transfection treated with the proteasome inhibitor MG132 for 20 h (+MG132) to enhance mature aggresome formation, or with DMSO, the vehicle control (−MG132). Subsequently, cells were fixed and immunostained with anti-dynein antibodies (red) and analyzed by fluorescence microscopy for colocalization (yellow). (E) Colocalization of GFP-250 aggresomes with HDAC6. HeLa cells transfected with GFP-250 (n=103 cells scored) were fixed and immunostained with anti-HDAC antibodies (red) and analyzed for colocalization (yellow) by fluorescence microscopy. (F) Colocalization of v-ErbA aggresomes with HDAC6. HeLa cells transfected with GFP-v-ErbA (n=100 cells scored) were fixed and immunostained with anti-HDAC antibodies (red) and analyzed for colocalization (yellow) by fluorescence microscopy.

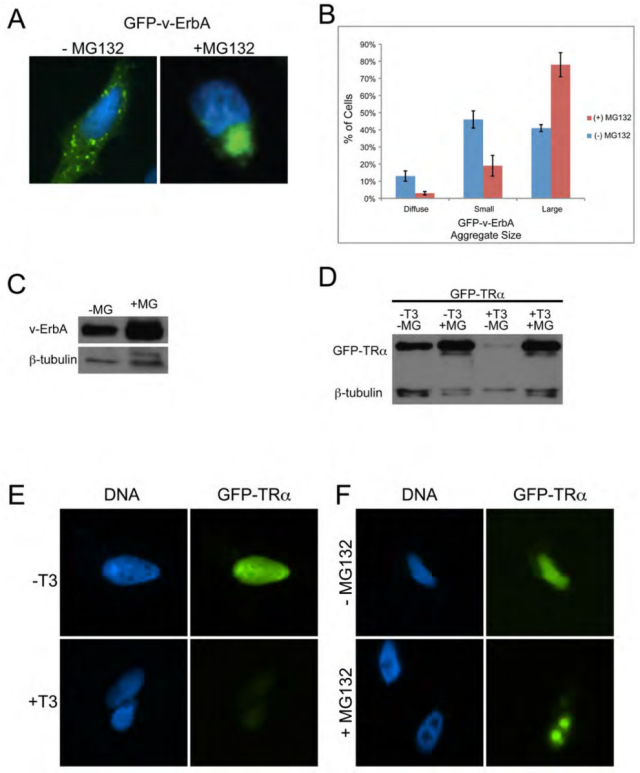

Fig. 5.

Proteasome inhibition increases v-ErbA aggregate size but does not induce TRα1 cytoplasmic foci. (A) To determine whether the size of v-ErbA foci would increase in response to proteasome inhibition, 16 h post-transfection, HeLa cells expressing GFP-v-ErbA were treated with the proteasome inhibitor MG132 for 20 h (+MG132), or with DMSO, the vehicle control (−MG132). Most of the large aggregates were spherical in morphology and coalesced into a single aggregate. (B) Bar graph summarizing the effect of MG132 treatment on v-ErbA aggregate size. There was a significant shift in frequency distribution from smaller aggregates to large aggregates ($p < 0.001$; n=2 replicate transfections, 200 cells scored). Error bars indicate ±SEM. (C) HeLa cells were transfected with expression vector for GFP-v-ErbA, in the presence (+MG) or absence (−MG) of the proteasome inhibitor MG132, as indicated. Forty-eight hours post-transfection, whole cell extracts were subject to Western blot analysis using anti-GFP antibodies, and anti-β-tubulin antibodies as an internal recovery control. Bio-Rad pre-stained Kaleidoscope protein molecular mass standards were used to confirm protein identity (GFP-v-ErbA, 102 kDa; β-tubulin, 55 kDa). (D) The proteasome mediates degradation of TRα1. HeLa cells were transfected with expression vector for GFP-TRα1, in the presence (+T3) or absence (−T3) of thyroid hormone and/or in the presence (+MG) or absence (−MG) of the proteasome inhibitor MG132, as indicated. Forty-eight hours post-transfection, whole cell extracts were subject to Western blot analysis using anti-GFP antibodies, and anti-β-tubulin antibodies as an internal recovery control. Bio-Rad pre-stained Kaleidoscope protein molecular mass standards were used to confirm protein identity (GFP-TR, 73 kDa; β-tubulin, 55 kDa). (E) HeLa cells were transfected with expression vector for GFP-TRα1. 24 h post-transfection,

cells were fixed and analyzed by fluorescence microscopy. In the absence of thyroid hormone (−T3) fluorescence intensity was typically greater than in the presence of thyroid hormone (+T3). Images were captured using the same exposure times. (F) HeLa cells were transfected with expression vector for GFP-TRα1. After treatment with MG132 or DMSO, the vehicle control, cells were fixed and analyzed by fluorescence microscopy. In the presence of MG132 (+MG132), fluorescence intensity was typically much greater than in the absence of MG132 (−MG132), and some cells showed nuclear aggregates of TRα1.

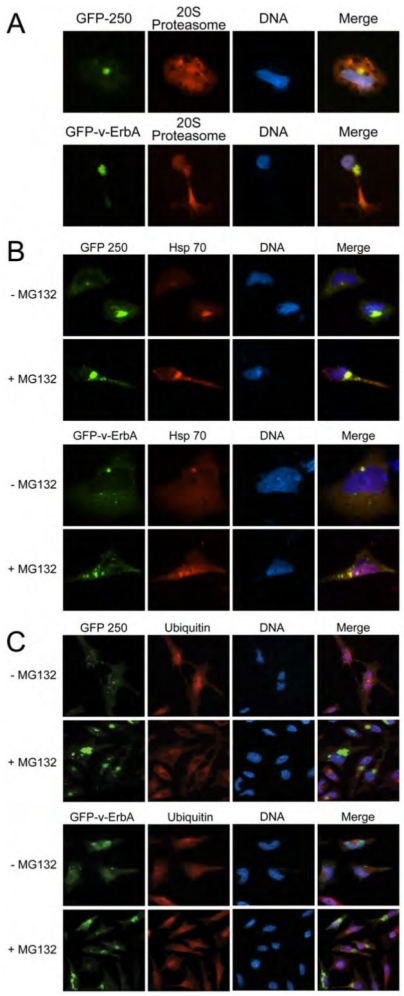

Fig. 6.

v-ErbA foci colocalize with 20S proteasome subunits and Hsp70 but not with ubiquitin. (A) Colocalization of 20S proteasome subunits with GFP-250 and v-ErbA aggresomes. HeLa cells overexpressing GFP-250 (upper panels) or GFP-v-ErbA (lower panels) were fixed 48 h post-transfection and immunostained with anti-20S proteasome antibodies (red). In the merged images, yellow indicates colocalization; blue, nuclei stained with DAPI. (B) Colocalization of Hsp70 with GFP-250 (upper set of panels) and v-ErbA (lower set of panels) aggresomes. HeLa cells overexpressing GFP-250 or GFP-v-ErbA were treated with the proteasome inhibitor MG132 (+MG132) to enhance aggresome formation, or with DMSO (vehicle control, −MG132), then fixed and immunostained with anti-hsp70 antibodies (red). In the merged images, yellow indicates colocalization; blue, nuclei stained for DNA with DAPI. (C) Ubiquitin does not colocalize with GFP-250 (upper set of panels) and v-ErbA (lower set of panels) aggresomes. HeLa cells overexpressing GFP-250 or GFP-v-ErbA were treated with the proteasome inhibitor MG132 (+MG132) to enhance aggresome formation, or with DMSO (vehicle control, −MG132), then fixed and immunostained with anti-ubiquitin antibodies (red).

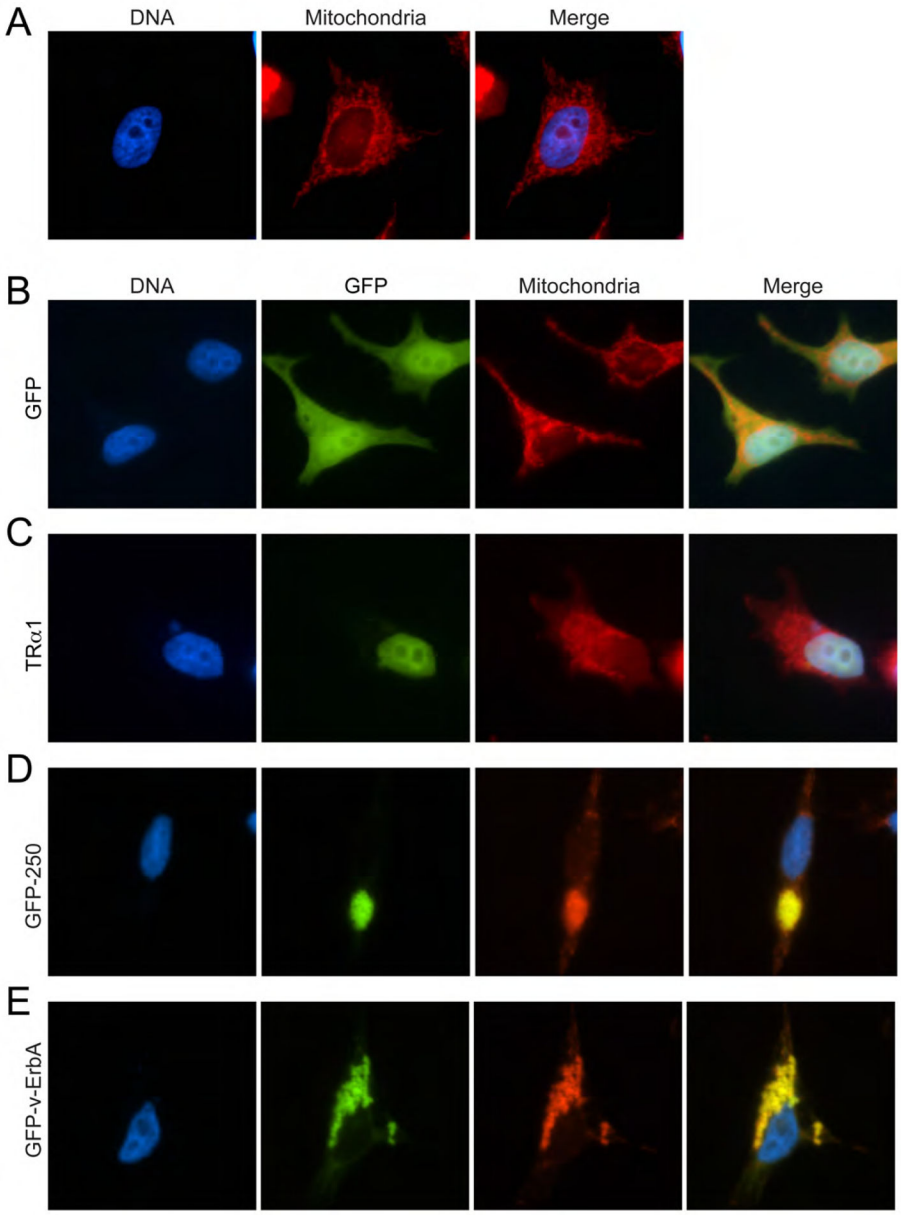

Fig. 7.

Mitochondria are recruited to v-ErbA aggregates. In untransfected cells (A), and in cells transfected with expression vectors for EGFP (B) and GFP-TRα1 (C) as controls, mitochondria were distributed throughout the cytosol. Untransfected or transfected HeLa cells were stained with MitoTracker Red to visualize mitochondria, then fixed and analyzed by fluorescence microscopy. Blue, nuclei stained for DNA with DAPI. In cells transfected with expression vectors for GFP-250 (D) or GFP-v-ErbA (E), mitochondria were retracted from the cell periphery and colocalized with aggresomes. In the merged images, yellow indicates colocalization.

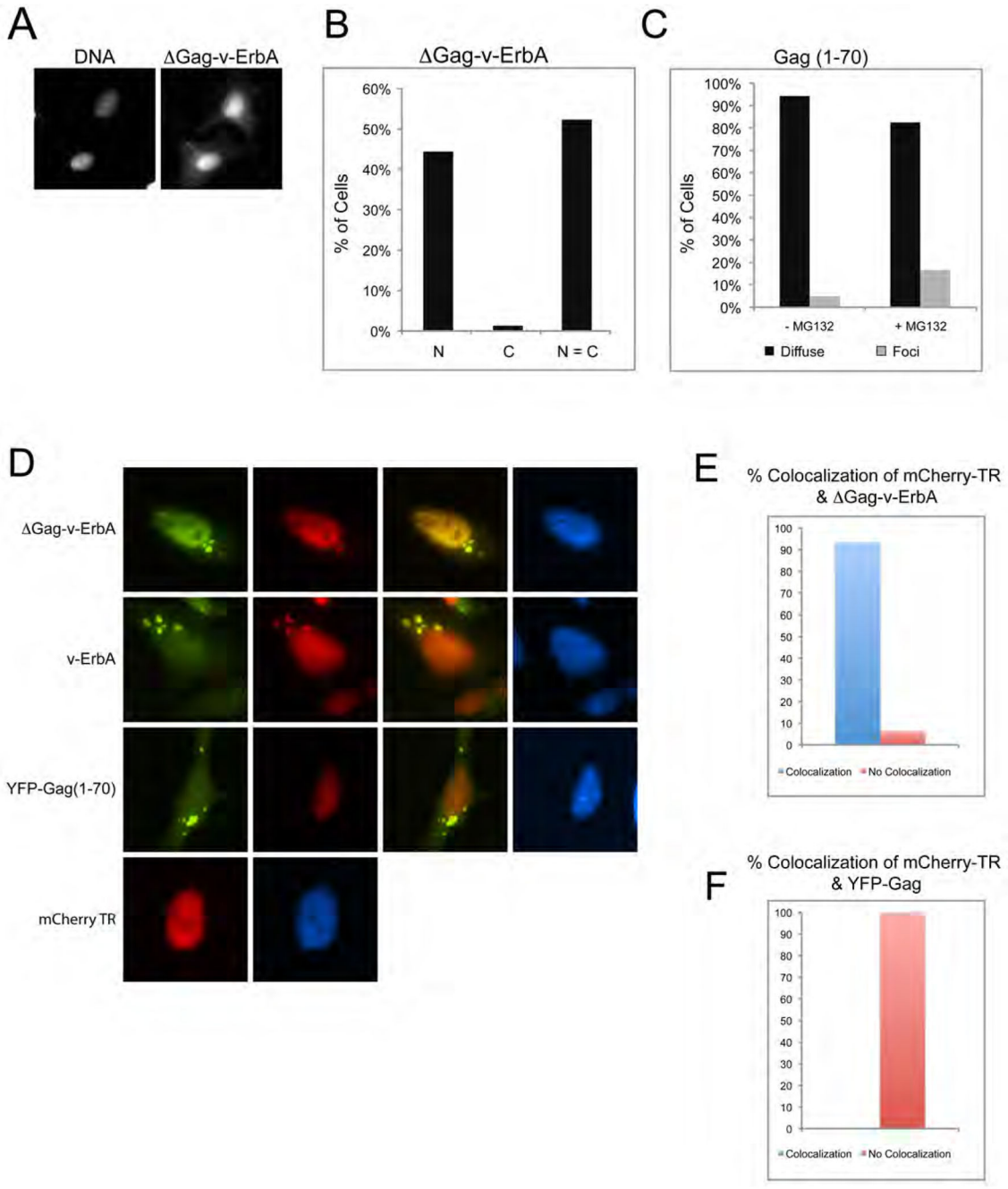

Fig. 8.

The AEV Gag sequence plays a role in targeting of v-ErbA to aggresomes. (A) HeLa cells were transfected with expression vectors for GFP-ΔGag-v-ErbA (deletion of Gag sequence). 24 h post-transfection, cells were fixed and analyzed by fluorescence microscopy. A representative example of the subcellular distribution of GFP-ΔGag-v-ErbA is shown. GFP-ΔGag-v-ErbA was more nuclear than GFP-v-ErbA and had very few cytoplasmic aggregates compared with GFP-v-ErbA. Nuclei were stained for DNA with DAPI. (B) Bar graph summarizing the distribution pattern of ΔGag-v-ErbA. N, predominantly localized to the nucleus; C, predominantly localized to the cytoplasm; N=C, whole cell distribution (n=200

cells scored). (C–E) Colocalization of TRα1 in cytoplasmic foci containing v-ErbA or ΔGag-v-ErbA, but not Gag (1–70). (C) HeLa cells were co-transfected with expression vectors for mCherry-TRα1 and GFP-v-ErbA (with Gag sequence), GFP-ΔGag-v-ErbA, or YFP-Gag (1–70). 24 h post-transfection, cells were fixed and analyzed for co-localization by fluorescence microscopy in cells with prominent cytoplasmic foci. In the merged images, yellow indicates colocalization; blue, nuclei stained with DAPI. (D) Bar graph summarizing the percentage of cells in which mCherry-TRα1 and GFP-ΔGag-v-ErbA were colocalized (n=100 cells scored per treatment). (E) Bar graph summarizing the percentage of cells in which mCherry-TRα1 and YFP-Gag (1–70) were colocalized (n=100 cells scored per treatment).

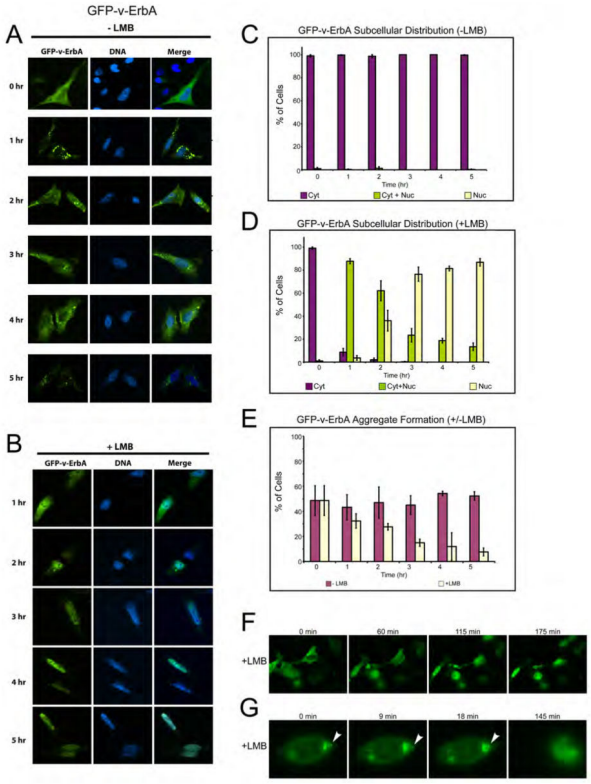

Fig. 9.

Dynamics of v-ErbA aggresome formation in the presence of leptomycin B (LMB). (A) In the absence of LMB (−LMB), v-ErbA has a predominantly cytoplasmic localization. HeLa cells were transfected with expression vector for GFP-v-ErbA. 16–20 h post-transfection, cells were treated for 0–5 h with vehicle (0.1% methanol), as indicated, fixed, stained for DNA with DAPI, and analyzed by fluorescence microscopy. (B) In the presence of LMB (+LMB), v-ErbA has a predominantly nuclear localization. HeLa cells were transfected with expression vector for GFP-v-ErbA. 16–20 h post-transfection, cells were treated for 1–5 h with leptomycin B (+LMB). (C) Bar graph summarizing the subcellular location of v-ErbA over time in the absence of LMB. Cyt, predominantly cytoplasmic; Cyt+Nuc, whole cell; Nuc, predominantly nuclear localization. (D) Bar graph summarizing the subcellular location of v-ErbA over time in the presence of LMB. (E) Bar graph summarizing the effect of LMB on v-ErbA aggregates over time. Error bars indicate ±SEM. (F–G) Time lapse imaging of dynamics of v-ErbA aggregates in single cells. HeLa cells were transfected with expression vector for GFP-v-ErbA. After 48 h, cells were subject to time-lapse imaging in the presence of LMB, with images acquired every 15 s for 6 h. Two Quick-Time movie files are attached as supplemental materials (Videos S1 and S2). (F) A panel of images from a cell with small aggregates, at time points indicated, during LMB treatment (see Video S1). (G) A panel of images from a cell with large aggregates, at time points indicated, during LMB treatment, ending in cell death (see Video S2). White arrowheads indicate movement of a small aggregate that coalesces with the large aggresome at the nuclear periphery.